
# SYNERGIES BETWEEN ALTERNATIVE FUELS AND AFTER TREATMENT SYSTEMS FOR EMISSIONS CONTROL - A SIMULATION STUDY

by

Fengzhe Wang

A thesis submitted to the University of Birmingham for the degree of
MASTER OF SCIENCE (RESEARCH)

Department of Mechanical Engineering
School of Engineering
University of Birmingham
February 2024

# ABSTRACT

Global warming is a growing issue, which countries and regions are tackling by the development of policies and technologies to reduce greenhouse gas emissions. One of the key initiatives is the promotion of Net-Zero emission solutions. The use of zero carbon (e.g. hydrogen ($H_2$), ammonia ($NH_3$) and carbon neutral (e.g. electrofuels) alternative fuels can contribute to reduce greenhouse gas emissions, while any unintended environmental impacts such as worsening of air quality due to local pollutants should be avoided. One of the main pollutants is nitrogen oxides (NOx), which are a major cause of air pollution and respiratory diseases. One of the most effective pathways to reduce NOx emissions is to use selective catalytic reduction (SCR) after treatment solutions. SCR commonly uses ammonia ($NH_3$) to convert NOx into harmless nitrogen gas, while there other types of SCR which also uses $H_2$ to reduce NOx. However, the efficiency of these after treatment systems is influenced by a number of factors, including emissions derived from different fuel types, combustion conditions and after treatment catalysts. In particular, emissions from the combustion process can affect the selectivity of SCR catalysts, leading to the generation of unwanted by-products such as nitrous oxide ($N_2O$) and ammonia slippage. Therefore, it is crucial to study the synergy of alternative fuels and after treatment systems. Based on the AVL Cruise M software, an after-treatment system model and an alternative fuel engine model is built. Through simulation under pure gasoline exhaust conditions, the ability of after treatment components to convert pollutants was studied; and by changing the fuel in the alternative fuel engine model, the impact of zero-carbon fuels ($H_2$ and $NH_3$), on engine emissions is analysed.

***Keywords:*** *Alternative fuels, After-treatment technology, Selectivity catalytic reduction, AVL Cruise M.*

# ACKNOWLEDGEMENTS

I would like to dedicate my lead supervisor Dr Jose Martin Herreros Arellano sincerely for his full support, patient guidance and kind help for not only my study but also my life in University of Birmingham. I would also like to thank my co-supervisors, Professor Athanasios (Thanos) Tsolakis and Dr Soheil Zeraati Rezaei, for their helpful advice and valuable support during this study. I am gratefully apricate Dr Omid Doustdar and Dr George Brinklow for giving me useful comments on my research topic and helping me with my experimental/simulation works.

I acknowledge AVL for providing access to its advance simulation technologies and software technical support within the frame of University Partnership Program.

I would like to thank my colleagues, Mr. Mengda Wu, Mr Mustafa Yavuz, Dr Alexis Cova Bonillo, Mr Andrew Norman for their technical help and support. I would like to express my gratitude to many friends as well, though not individually named here, their friendship and encouragement have played a significant role during my study.

I would like to deliver my heartfelt thanks to my girlfriend, Yaning Zhou. Thank you for bringing love and joy to my life and providing me with care and accompany.

Last but certainly not least, I want to dedicate this thesis to my warmly family. Thanks to my parents for inspiring me when times are tough, urging me on when things are going well, and for the sincere love and support you have given me over the years enabling me to follow my dreams.

# TABLE OF CONTENTS

# 1. INTRODUCTION

In recent years, the issue of global warming has become increasingly serious, and measures to reduce greenhouse gas emissions to mitigate the impact of climate change has become urgent. In this context, more and more countries and regions have begun to formulate emission reduction plans, and one of the key goals is to achieve Net-zero emissions. Alternative fuels are developed to achieve this target, however, the pollutants from these alternatives may have environmental impacts. Therefore, further studies are needed to assess their environmental effects and feasibility.

One of those pollutants is nitrogen oxides (NOx), which is a major contributor to air pollution and respiratory diseases. One of the most effective ways to reduce NOx emissions is by using a NOx after treatment system which employs a selective catalytic reduction (SCR) process that uses ammonia ($NH_3$) and/or hydrogen ($H_2$) to convert NOx to harmless nitrogen gas.

However, the efficiency of these after treatment systems is affected by several factors including fuel type, combustion conditions, and after treatment catalysts, etc. In particularly, emissions from the combustion process can affect the selectivity of the SCR catalyst, leading to the formation of unwanted by-products such as nitrous oxide ($N_2O$) and ammonia slip. Therefore, the synergy between alternative fuels and after treatment systems is significant for emission control of internal combustion engines.

The first objective of this study is to analyse the ability of TWC and SCR to treat and convert harmful components in the exhaust gas by testing the concentration of CO, $CO_2$, NO, $NO_2$, THC and other emissions before and after TWC and SCR catalysts under pure gasoline conditions in the simulation of the after treatment system, and to

develop a basic model of after treatment system for the study of synergies between alternative fuels and emission after treatment systems in the emission control of internal combustion engines. Another objective is to build a simulation model of an alternative fuel engine by using AVL Cruise M software and verify the feasibility of this model for engine emissions simulation by calibrating the engine parameters, combustion and emissions formation models. Furthermore, by introducing hydrogen and ammonia-hydrogen blended fuels and simulating the emissions of CO, NOx and THC under different hydrogen energy substitution ratios, the role of zero-carbon fuels on emissions of internal combustion engines is summarised, especially the effect of hydrogen and ammonia-hydrogen blended fuels on the emissions of gasoline GDI engines and their synergistic effect on after treatment systems to achieve emissions management.

In this study, an after treatment system and an alternative fuel engine are modelled in AVL Cruise M software, and the effects of the conversion ability of after treatment system on the components in the exhaust gas and the energy substitution ratio of the alternative fuel on the engine emission are investigated respectively. The feasibility of the model simulation is verified by comparing with the experimental data, and the results of conversion efficiency of catalysts and the effect of alternative fuel on exhaust gas provide insights for further development and design of zero-carbon fuel engines.

# 2. LITERATURE REVIEW

## 2.1 Alternative fuel technologies

### 2.1.1 Introduction

Alternative fuels are a fundamental way to reduce carbon emissions, and a variety of energy sources such as hydrogen, liquefied natural gas, biofuels, alcohols all have their own advantages and applications [1].

Natural gas is a blend of hydrocarbons including methane, ethane, propane, butane, and other higher alkanes. Apart from carbon dioxide, traces of hydrogen sulfide and nitrogen, there may also be small amounts of higher hydrocarbons like ethylene. Liquefied natural gas is a low-temperature liquid that is transparent, odourless, non-toxic, and non-corrosive at atmospheric pressure. The density of LNG is approximately 0.4-0.5 kilograms per liter, depending on temperature, pressure, and composition. It has a lower carbon content than coal or oil and offers opportunities for diversified energy supply. In comparison to CNG, LNG becomes a more viable option for long-distance transportation as LNG has distinct advantages such as ease of transport, storage, and better density than gaseous methane [2].

According to their physical states, alternative fuels can be categorized into solid, liquid, and gas. Liquid alternative fuels serve as a desirable alternative to conventional fuels in the industry of transportation due to high energy density in terms of mass and volume. Some of the major liquid fuels include bioethanol, biodiesel, and bio-oil. They have a higher oxygen content ranging from 10% to 45% compared to traditional fossil fuels. They have lower sulfur content and higher nitrogen content than petroleum-based sources, and they can be safely transported, stored, and modified. Additionally, advanced liquid biofuels offer additional advantages, such as reduced processing cost

and lower emissions of pollutants compared to fossil fuel engines, which have a significant impact on reducing emissions in the transportation sector [3]. However, this report will mostly focused on zero carbon fuels, in particular $H_2$ and $NH_3$.

### 2.1.2 Hydrogen

Hydrogen has been identified as a suitable alternative fuel to be used due to its high combustion efficiency and zero carbon content in its composition. Hydrogen is a colourless gas and can produce 142 kJ/g of heat once combusted. The only product of complete combustion of hydrogen is water, but NOx emissions cannot be avoided due to the involvement of nitrogen from air [4]. The main characteristics of hydrogen combustion includes wide ignition range, fast flame propagation speed and low ignition energy, and the heat release of hydrogen combustion in terms of mass is approximately three times higher than gasoline [5].

However, in practical use, the cost, safety, storage, and transportation of hydrogen are issues that need to be addressed. Additionally, the combustion of hydrogen produces nitrogen oxides as byproducts, which also need to be tackled in future research. Therefore, research efforts are required to achieve a hydrogen-based economy [6].

### 2.1.3 Ammonia

Due to the certain danger and high cost of hydrogen storage, the use of ammonia for transport applications has become a new research direction. Ammonia is colourless but irritating, and is gaseous above -33.5 degrees Celsius, which does not contain carbon, hence the products only contain water and nitrogen when burnt completely [7], [8]. Ammonia is composed of hydrogen and nitrogen. It contains 17.8% of hydrogen by mass, has thermal properties similar to propane and can be used as a hydrogen and energy carrier [8]. Compared to hydrogen, ammonia is cheaper to store energy,

has a comparable volumetric energy density to gasoline, is easier to produce, handle and distribute, and is more commercially viable.

However, there are challenges of $NH_3$ for new engine applications that should be understood and overcome. $NH_3$ has a high autoignition temperature, low flame propagation speed and narrow flammability limits hindering high $NH_3$ energy replacement rates with acceptable combustion quality and $NH_3$ slippage to levels suitable for the catalytic technologies to deal with. $NO_X$ – $N_2O$ - $NH_3$ trade-offs have been identified in $NH_3$ combustion and exhaust after-treatment systems. Tailored exhaust after-treatment catalytic technologies are required and further trade-offs between primary and secondary emissions should be identified and resolved. $NH_3$ is a zero carbon fuel producing zero $CO_2$ tailpipe emissions. However, greenhouse gas footprint should be evaluated from a “well to wheel” perspective in order to unveil the full decarbonisation potential. Due to the challenges related to $NH_3$ combustion, the use of $H_2$ and/or pilot/promoter fuels are some of the approaches which could be used to enhance $NH_3$ reactivity. For instance, ammonia autothermal reforming ($NH_3$-ATR) has been studied combining with selective oxidation of ammonia and ammonia thermal decomposition. It is proved that the feasibility of ammonia exhaust gas reforming as a source of hydrogen fuels is valid. It uses diesel engine exhaust gas as the oxygen source and achieves hydrogen production by controlling parameters such as oxygen/ammonia ratio and inlet gas velocity. In addition, the reforming product is added to internal combustion engines and the results show that the use of ammonia exhaust gas reforming can effectively reduce engine carbon emissions [9]. Therefore, the study of the effects of ammonia-hydrogen combustion emissions on the performance of NOx after treatment systems, especially SCR catalysts, is also crucial.

## 2.2 Ammonia/Hydrogen engines

### 2.2.1 CI dual-fuel engines with $NH_3/H_2$

Compression-ignition engines do not rely on spark plugs to ignite but cause the mixture to spontaneously ignite by compressing to the high temperature and high pressure in the top front cylinder, and the compression ratio is usually higher than that of SI engines. Due to the limitation of the ignition method, the ammonia-hydrogen fuel substitution ratio of the compression ignition engine generally cannot reach 100%, and the dual-fuel mode of ammonia and/or hydrogen mixed with traditional diesel is usually adopted.

In ammonia/diesel dual fuel compression ignition engines, ammonia can provide about 84.2% of the input energy, while increasing the energy replacement ratio is able to enhance the indicated thermal efficiency and change the combustion mode from pure diesel diffusion combustion to premixed combustion in a dual fuel mode. Although ammonia can substantially decrease $CO_2$, CO and particulate matter emissions, NOx and ammonia slips (14,800 ppm) are increased due to higher concentration of nitrogen in fuel and incomplete combustion. In addition, in order to reduce greenhouse gas (GHG) emissions, it is necessary to replace diesel fuel with more than 35.9% ammonia, as ammonia combustion produces $N_2O$ (90 ppm), which offsets the reduction in $CO_2$ [10]. However, ammonia has a significant inhibiting effect on the spontaneous combustion of the pre-ignited fuel, and increasing the proportion of ammonia substitution increases the ignition delay time and leads to an increase in the intensity of premixed combustion, so the injection strategy needs to be optimised to achieve lower emissions while maintaining higher efficiency [11]. The high-pressure injection dual fuel mode can offset the poor combustion characteristics of ammonia fuels and

has the potential to replace 97% diesel in blended fuel, while significantly reducing equivalent $CO_2$ emissions with a slight increase in ammonia emissions [12].

An injection timing(IT)-coupled with diesel energy fraction strategy in the ammonia-diesel stratified injection (ADSI) mode can reduce indicated specific fuel consumption and GHG by approximately 4% and 94% respectively, achieving a combustion efficiency of over 99% and limiting unburned ammonia to less than 150 ppm [13].

The use of ammonia as a fuel remains challenging, but given that $NH_4NO_2$ can reduce the compression ignition boundary of ammonia and that mixed with hydrogen or mixed with ammonium nitrate will revise the ignition performance of ammonia, $NH_3/NH_4NO_2$ and $NH_3/H_2$ blends could be potential fuels, but further research and improvements are needed [14]. Simulations of $NH_3/H_2$ combustion with diesel fuel show that it can achieve higher energy conversion efficiency than diesel fuel [15]. In addition, the use of ammonia and hydrogen combustion to improve $CO_2$ emissions from diesel engines and the introduction of a new oxidising fuel, DGE, can improve combustion efficiency and reduce unburned $H_2$ and $NH_3$ emissions, and replacing 60-70% of diesel fuel with DGE, $H_2$ and $NH_3$ can reduce $CO_2$ emissions by 50%. At the same time, there are synergies between DGE and gaseous fuels for example hydrogen and ammonia, which can concurrently reduce harmful emissions such as PM, NOx, HC and CO [16].

### 2.2.2 SI dual-fuel engines with $NH_3/H_2$

As a renewable carbon-free fuel, hydrogen/ammonia is considered a potentially excellent alternative fuel in internal combustion engines. The combustion instability and ignition problems of ammonia in internal combustion engines limit its large-scale application [17], but as $H_2$ and $NH_3$ have opposite and complementary combustion properties, it is logical and with great potential to co-combust ammonia with hydrogen

[18]. The ammonia and hydrogen blended fuel increases the compression ratio and thus the efficiency and power compared to petrol.

Waste exhaust heat can be used to decompose $NH_3$ into $H_2$, $N_2$ with some unconverted $NH_3$ depending on the specific reaction conditions [19]. The addition of $H_2$ into $NH_3$ combustion improves power output and indicated efficiency. Hydrogen is primarily used as an ignition booster rather than a global combustion booster. Small amounts of hydrogen and overboost operation can greatly improve engine performance and stability, making ammonia a well-suited fuel for spark ignition engines. In addition, hydrogen can reduce unburned ammonia emissions [20]. The addition of a low quantity of hydrogen effectively alleviates the drawbacks of ammonia combustion. Further addition of hydrogen exacerbates the decline in apparent thermal efficiency because of higher heat transfer losses due to high temperature hydrogen combustion [17]. Under lean combustion conditions, the addition of small percentages of ammonia into gasoline combustion reduces the rate of combustion of the blended fuel, extending the period of flame development and propagation of the engine, and decreasing the in-cylinder pressure and peak heat release rate. The addition of ammonia increases the peak indicated mean effective pressure and thermal efficiency, but results in increased nitrogen oxide (NOx) emissions (mainly fuel derived) [21].

Both ammonia and hydrogen have a higher octane rating than gasoline, allowing them to run at higher compression ratios. The combustion rates and minimum ignition energies of ammonia and hydrogen differ considerably, and a suitable compromise can be obtained by mixing them. The ratio of ammonia to hydrogen can be used as a new potential engine control parameter [19]. At different compression ratios, with the proportion of hydrogen mixture to total fuel energy varying from 5 to 21%, an increase

in compression ratio leads to faster flame development, faster flame propagation and shorter combustion progress. By the same measure, increasing the hydrogen concentration can enhance combustion, resulting in a quick increase in pressure and temperature [19]. At 1400 and 1800 rpm, an increase in hydrogen content from 5% to 21% results in a 13.64% decrease in volumetric efficiency, but a 16.89% and 33% increase in fuel efficiency and thermal efficiency respectively. The retarded combustion characteristics of ammonia prolongs the combustion time, resulting in higher exhaust temperatures at lower hydrogen contents. As hydrogen content and compression ratio increase, this effect diminishes, and exhaust temperatures decrease. Increasing the hydrogen content increases the peak temperature and therefore NOx emissions continue to increase despite the reduction in ammonia (mainly thermal NOx). For NOx control due to ammonia/hydrogen blends, selective catalytic reduction (SCR) could be a practical solution [22].

As an energy carrier and primary fuel, the use of direct hydrogen injection has proven to achieve high power output and efficiency with low emissions for spark ignition internal combustion engines due to its carbon free content, wide combustion limits and fast flame speed. However, further research and technological development is needed to achieve its wider application [5]

## 2.3 After treatment technologies

### 2.3.1 Three Way Catalysts

The three-way catalyst is an after treatment device that has been used commercially on a large scale. It is generally made of porous ceramics or materials such as $Al_2O_3$ as the carrier, which itself does not participate in catalytic reactions. Normally, the

precious metals such as Pt, Rh, and Pd are used as the active components. When the high temperature exhaust gas passes through the devices, the activities of CO, HC, and NOx will be enhanced, resulting in a simultaneous oxidation-reduction chemical reaction, in which CO is oxidised to colourless and non-toxic $CO_2$ and HC is oxidised to water and $CO_2$, and NOx is reduced to $N_2$ and $O_2$, so as to reduce the emission of hazardous gases. TWC has a high conversion efficiency within a certain air-fuel ratio range, but cannot achieve a high NOx conversion rate under rich and lean combustion conditions [23].

### 2.3.2 SCR technologies

Nitrogen oxide emissions from engines have a detrimental effect on human health and the environment, which are exacerbated by the increased use of diesel engines [24] and nitrogen-containing alternative fuels. Methods of reducing nitrogen oxide (NOx) and particulate matter (PM) emissions include alternative fuels, pre-combustion methods, in-cylinder methods and after treatment systems. A combination of pre-combustion, in-cylinder and after treatment methods coupled with alternative fuel technologies can be effective in reducing NOx and PM emissions [25]. With the introduction of stricter emission standards, NOx after treatment systems have had to be used to control NOx emissions to meet emission regulations, with technologies such as SCR, SNCR (Selective Non-Catalytic Reduction) and LNT. Of these technologies, SNCR does not require a catalyst and can achieve NOx emission reduction levels of only around 50%; the LNT method provides low temperature activity through adsorption of NOx, but is limited at high temperatures and the cost of the catalyst is expensive [24].

SCR technology is most effective in denitrification, with a low impact on engine dynamics and fuel economy, and the development and research of related catalysts is well established and operating costs are low, so SCR technology has a strong applicability and versatility [26]. The most common SCR technology to remove NOx is mainly through $NH_3$-SCR, while $H_2$-HCR is in research stage. The indicators of reaction catalyst performance are $N_2$ selectivity and the rate of NOx conversion. Catalysts are being developed and evaluated under ideal gas conditions in the laboratory, which provides selection basis of catalyst to be effective under real exhaust gas conditions.

**$NH_3$-SCR**

The SCR reaction has overall three different reaction pathways under three different conditions, depending on the concentration ratio of NO to $NO_2$: When no nitrogen dioxide is present in the gas mixture, nitric oxide (NO) reacts with $NH_3$ in the presence of oxygen via the "standard SCR" reaction shown in Eq. (1). When nitrogen dioxide and nitric oxide are present at the same time, NO and $NO_2$ react with $NH_3$ at a concentration ratio of 1:1 through the "fast SCR" reaction shown in Eq. (2). If the concentration of $NO_2$ far exceeds NO, $NO_2$ and $NH_3$ react according to the "$NO_2$-SCR" path shown in Eq. (3). [27].

$$4NO + 4NH_3 + O_2 \rightarrow 4N_2 + 6H_2O \quad (1)$$

$$NO + NO_2 + 2NH_3 \rightarrow 2N_2 + 3H_2O \quad (2)$$

$$6NO_2 + 8NH_3 \rightarrow 7N_2 + 12H_2O \quad (3)$$

Figure 1 and figure 2 show the NOx conversion and $N_2$ selectivity of different catalysts in the $NH_3$-SCR reaction under different experimental conditions, and Table 1 shows the corresponding experimental conditions [28-31].

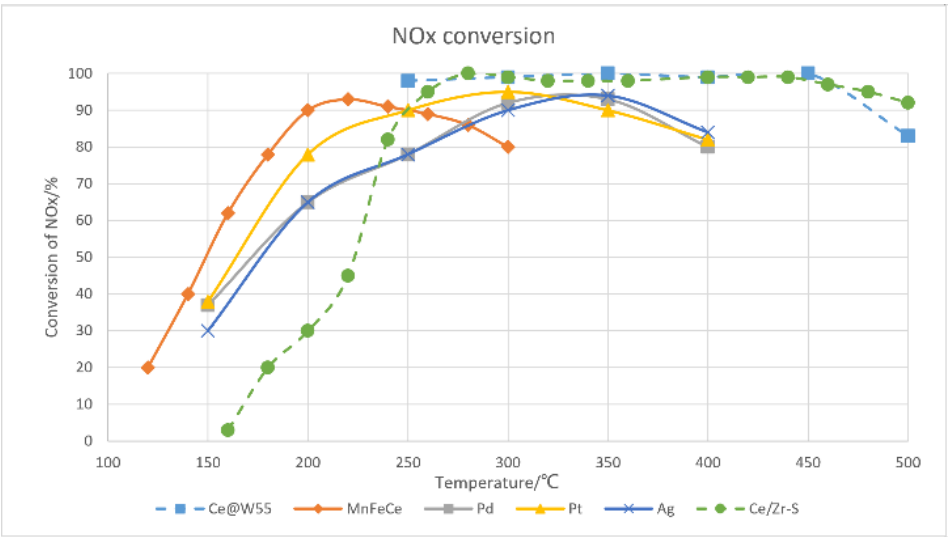


Figure 1 NOx Conversion efficiency with temperature for several $NH_3$-SCR after treatment catalysts

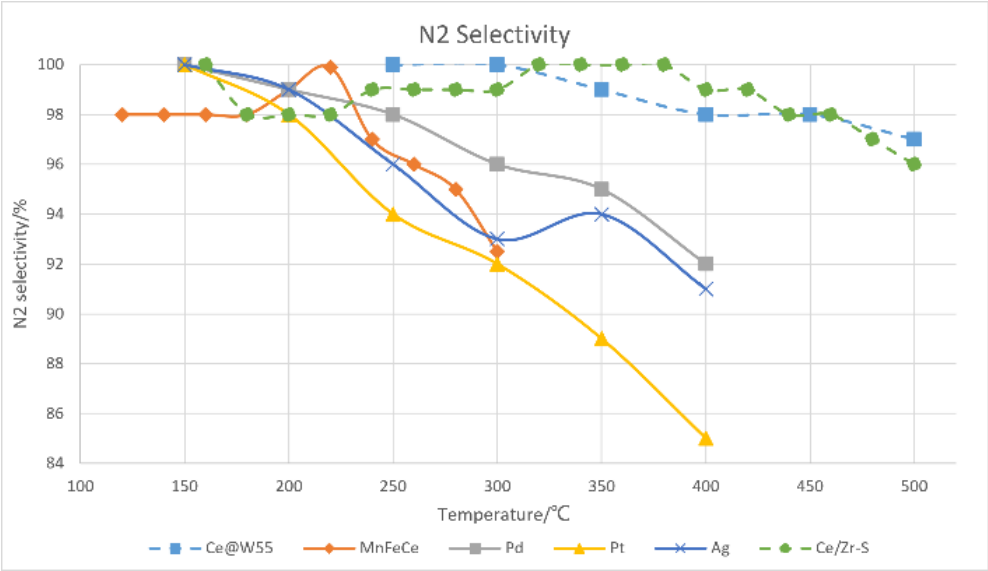


Figure 2 $N_2$ Selectivity with temperature for several $NH_3$-SCR after treatment catalysts

Table 1 Experimental Conditions

| Catalyst | Conditions | | | | |
|---|---|---|---|---|---|
| | NO (ppm) | $NH_3$ (ppm) | $O_2$ | $H_2O$ | GHSV（h-1） |
| Ce@W55 | 500 | 500 | 5% | 5% when used | 176,000 |
| MnFeCe | 600 | 600 | 5% | 10% when used | 100,000 |
| Ag | 50 | 50 | 4% | | 40,000 |
| Pt | 50 | 50 | 4% | | 40,000 |
| Pd | 50 | 50 | 4% | | 40,000 |
| Ce/Zr-S | 500 | 500 | 5% | | 30,000 |

As shown in Figure 1 and figure 2, the above catalysts generally had high NOx conversions from 200 °C to above 250 °C and were able to maintain more than 80% NOx conversion until 400 °C. However, as the temperature increased, there was a significant decrease in the nitrogen selectivity, except for the Ce catalyst. One of the better performing $CeO_2$@$WO_3$ core-shell structured catalysts is not only more tolerant to $SO_2$ and $H_2O$, but also achieves approximately 100% NOx conversion and $N_2$ selectivity over a wider activity temperature window of 250-450 °C.

For other catalysts the performance disadvantage can also be weakened after modifying to achieve near ideal deNOx capability. The addition of $H_2$ to Ag/$Al_2O_3$ catalysts can increase $NO_2$ production, thus increasing the activity of the $NH_3$-SCR reaction and effectively reducing NOx concentrations, but this approach increases fuel economy and $CO_2$ emissions. Alternatively, placing Pt/$Al_2O_3$-DOC before SCR or adding $H_2$ before DOC and SCR can also increase the concentration of $NO_2$ and thus promote the $NH_3$-SCR reaction [32]. Besides, in a "fast SCR" mechanism, i.e. in the presence of ammonia, hydrogenation can also improve the NOx catalytic activity of Ag/$Al_2O_3$ catalysts [33].

Ag/$Al_2O_3$ catalysts have moderate sulphur tolerance at low temperatures but can be regenerated at 670 °C in the presence of $H_2$, with the high temperature in diesel particulate traps [34]. The starting temperature of catalyst can be reduced by about 10 °C by adding Ti or Si [35].

Studies on the selective catalytic reduction of NOx at low temperatures with hybrid catalytic systems of metal oxides and Cu or Fe exchanged zeolite fractions suggest that hybrid catalytic systems are a potential improvement in SCR of NOx and may improve the efficiency of SCR catalysts under low temperature [27]. In a study of Cu,Fe/Beta catalysts, adding iron can slightly improve $NH_3$-SCR activity, $N_2$ selectivity and hydrothermal stability. At higher reaction temperatures, iron significantly improved the NOx conversion and $N_2$ selectivity of the hydrothermally aged Cu,Fe/SSZ-13 catalyst in the presence of propylene [36].

**$H_2$-SCR**

Low-temperature $H_2$-SCR is considered a potential alternative to existing $NH_3$-SCR and hydrocarbon denitrification (HC-SCR) technologies [37]. $H_2$-SCR is a promising DeNOx technology using $H_2$ as the reducing agent and precious metal catalysts (e.g. Pt-based and Pd-based catalysts) or non-precious metal catalysts for NOx removal [38], with the advantage of low operating temperature and high NOx removal efficiency [39]. For $H_2$-SCR catalytic reaction system, reactions shown in Eq. (4)- Eq. (6) are considered.

$$2NO + 4H_2 + O_2 \rightarrow N_2 + 4H_2O \quad (4)$$

$$2NO + 3H_2 + O_2 \rightarrow N_2O + 3H_2O \quad (5)$$

$$H_2 + 1/2O_2 \rightarrow H_2O \quad (6)$$

Figure 3 and figure 4 show the NOx conversion and $N_2$ selectivity of different catalysts in $H_2$-SCR reaction under different experimental conditions, and Table 2 shows the corresponding experimental conditions [40-45].

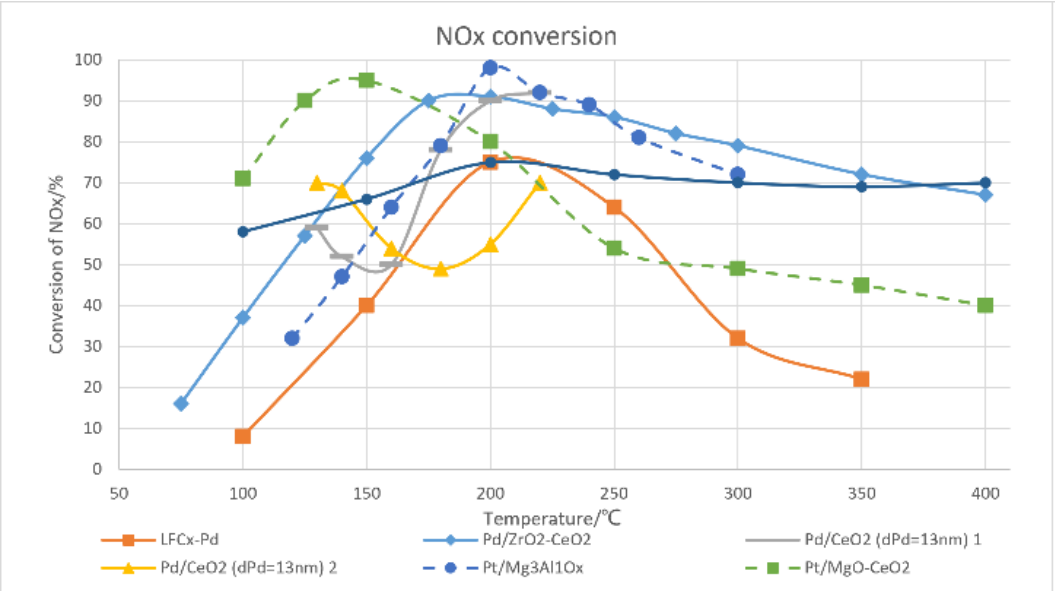


Figure 3 NOx Conversion efficiency with temperature for several $H_2$-SCR after treatment catalysts

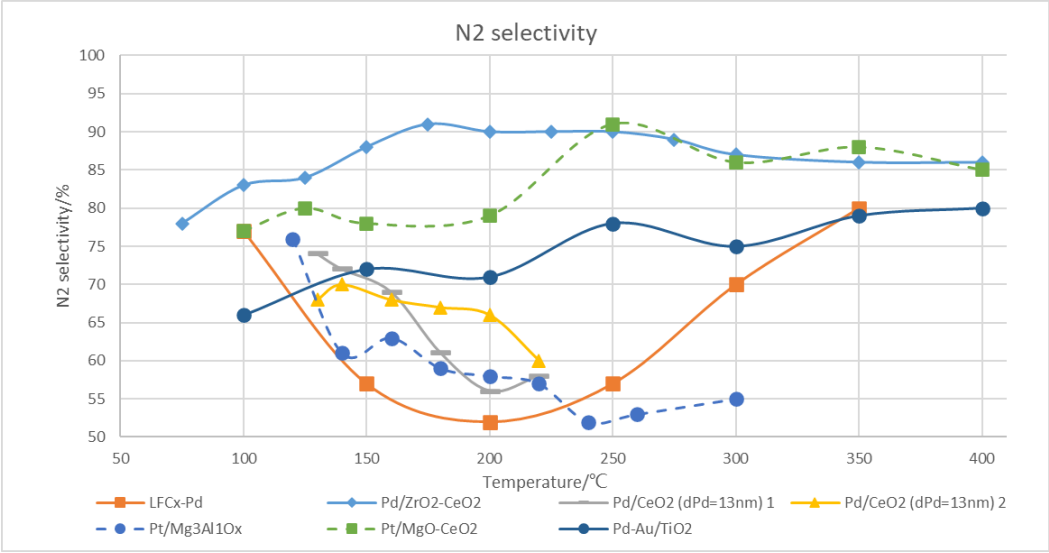


Figure 4 $N_2$ Selectivity with temperature for several $H_2$-SCR after treatment catalysts

Table 2 Experimental Conditions

| Catalyst | Conditions | | | | |
|---|---|---|---|---|---|
| | NO | $NO_2$ | $H_2$ | $O_2$ | GHSV（h-1） |
| LFCx-Pd | 0.072l% | | 1% | 5% | Not Given |
| $Pd/ZrO_2$-$CeO_2$ | 1000ppm | | 4000ppm | 6% | Not Given |
| $Pd/CeO_2$ | 340ppm | | 1% | 2.20% | 40,000 |
| Pd-$Au/TiO_2$ | 0.25% | | 1% | 5% | Not Given |
| $Pt/Mg_3$Al1Ox | 500 | | 1% | 5% | 120000 |
| Pt/MgO-$CeO_2$ | 0.25% | | 1% | 5% | 80,000 |

$H_2$-SCR exhibits higher NOx removal capability than $NH_3$-SCR in the low temperature range (100-200 °C). High NOx conversion and $N_2$ selectivity in the 100-200 °C range can be achieved using Pt/MgO-$CeO_2$ catalysts and still show good stability in the presence of $SO_2$. But NOx reduction decreases with increasing reaction temperature, while $NO_2$ production increases [46]. Modifications to the catalyst can help to improve NOx conversion. The addition of 1 wt.% tungsten to the Pt/HZSM-5 catalyst can significantly improve the activity and $N_2$ selectivity of the Pt/HZSM-5 catalyst in the $H_2$-SCR. The mechanism of tungsten is to accelerate the dissociation reaction of NO and $H_2$ on the Pt surface by promoting the metallisation state of Pt, which effectively inhibits the generation of unfavourable nitrate substances [47]. The use of polyvinylpyrrolidone (PVP) to orient ultrafine Pt particles on Beta zeolite can effectively control the particle size and dispersion of Pt particles, thus improving the NO conversion efficiency of the catalyst [48]. A titanium modified MCM-41 carrier can achieve a NOx conversion of about 89% and a $N_2$ selectivity of about 79% at a high GHSV (80,000 h/C01) of 1000 ppm NO, 5000 ppm $H_2$, 6.7% $O_2$ at low temperatures. At the same time, the catalyst is well tolerated for 20 ppm $SO_2$ or 50 ppm CO [49].

The surface properties and activity of the noble metal catalyst have a significant impact on the catalytic efficiency, matching the ability of catalyst to activate $H_2$ and adsorb NOx is very important for $H_2$-SCR catalysts [50]. For example, the introduction of cations that can accept more NOx species in the molecular sieve channel to match the NOx adsorption capacity with $H_2$ activation properties, such as $Al_3$+, can effectively improve catalytic performance [51]. Cr has a catalytic effect on the $H_2$-SCR reaction of Pt/ZSM-35 catalysts in excess oxygen. The addition of Cr not only enhances the adsorption of NOx but also promotes the formation of NH4+ species on the surface [52].

In addition, $H_2O$ has a positive effect on the conversion of $H_2$ but a different effect on the conversion of NOx. Below 120 °C, $H_2O$ promotes the conversion of NOx, while at higher temperatures it inhibits the conversion of NOx, this effect depends on the reaction temperature and the properties of the catalyst [53].

The Pd catalysts have a higher NOx conversion at low temperatures, but a lower nitrogen selectivity. The Pd/ Na-$TiO_2$ catalysts shows a higher catalytic activity and a wider activity temperature window in the $H_2$-SCR reaction，with the addition of Na. Taking Pd0.5Na0.5/Ti as an example, its activity is high and the NOx conversion can be maintained above 70% between 125 and 300 °C. Excessively low Na content clearly increases the NOx conversion, while excessively high Na content leads to a decrease in activity. The promotion of $N_2$ selectivity is not obvious below 250 °C, but

becomes obvious above 250 °C [54]. The use of lanthanum as a promoter, added to a palladium catalyst can improve $N_2$ selectivity and increase NOx conversion [55]. Palladium-Nickel/$TiO_2$ catalysts have a synergistic effect in the $H_2$-SCR reaction, with the addition of nickel enhancing the rate and distance of hydrogen spillover, improving catalyst activity and $N_2$ selectivity, while also promoting the formation of species that can actively adsorb NOx [56].

In addition to the common catalysts mentioned above, Ag/$Al_2O_3$ catalysts are less likely to be poisoned by nitrates [57]. Fe in the LaNi1/C0xFex$O_3$ catalyst (x=0.0, 0.2, 0.4, 0.7 and 1.0) can also contribute to the NOx removal efficiency and improve the stability of the catalyst [58].

To sum up, the laboratory experiments of $NH_3$-SCR and $H_2$-SCR catalysts under ideal exhaust gas composition discusses the synthesis methods and catalyst performance of different catalysts and provides a basis for catalyst selection for subsequent tests under real exhaust gas conditions. $NH_3$-SCR technology is not only investigated in the laboratory, but is also used in real vehicles, thus research on the application of $NH_3$-SCR for real vehicles is also ongoing. Ag/$Al_2O_3$ and Fe-BEA catalysts, individually or in combination, can be used to remove NOx from diesel engine with $NH_3$-SCR, The combination of Ag/$Al_2O_3$ and Fe-BEA at temperatures below 270 °C can work for low-temperature $NH_3$-SCR, but further optimisation of the catalyst capacity, the amount of $H_2$ fed and the NOx storage capacity is required [59].

The DOC+SCR after treatment device combination is available for ammonia/diesel dual fuel engines, where the NOx conversion efficiency of SCR is affected by the $NH_3$/NOx ratio and temperature, The key to this technology is to avoid the $N_2O$ emission due to the oxidation of $NH_3$, so that the conversion efficiency of SCR to $N_2O$ has a great impact on the GHG emission of vehicle [60].

## 2.4 Zero and One dimensional system level simulations

Achieving decarbonisation targets for clean road vehicles has become a focus for researchers, particularly in terms of achieving a reduction in the negative environmental and human health impacts of pollutants from conventional internal combustion engine emissions through the synergy of low and zero carbon alternative fuels and after treatment systems. This section provides a literature analysis of modelling of engine emissions and after treatment systems.

An early approach to using AVL Cruise software to predict vehicle performance, fuel economy and $CO_2$ emissions was proposed by Srinivasan et al. [61]. A simulation model of a production vehicle was built through different stages of the vehicle development process and validated by detailed comparison with experimental data. The validation includes a comparison of acceleration performance, driving performance, average fuel consumption and $CO_2$ emissions under typical driving cycles (UDC, EUDC). As a result, simulation technologies are verified to analyse the effects of vehicle characteristics and power parameter adjustments on fuel economy

and driving performance and demonstrate that it is a powerful and effective tool for identifying the modifications required to achieve vehicle performance and $CO_2$ emission targets. Wheeler et al. [62] used 1D model to obtain the optimum intake and exhaust timing, compression ratio and parameters of turbo charger, and used vehicle simulation to identify fuel economy improvements from the new engine design and advanced combustion control. Pacheco et al. [63] has taken similar modelling process to demonstrate the application and effectiveness of the HCCI combustion method in passenger cars, as well as their technical challenges and solutions.

Salek et al.[64] analysed the combustion process numerically using a validated numerical model of a naturally aspirated SI engine using the Vibe two-zone combustion model developed in AVL BOOST software. It was found that inlet injection of ammonia significantly reduces NOx emissions by approximately 50% over the entire engine speed range, but has some negative effects on fuel consumption rates, carbon monoxide and hydrocarbon emissions. Also with AVL Boost, Van et al.[57] simulated the performance and emissions of a large cargo ship's main engine through numerical thermodynamic simulations and performed special adaptations for marine engines and heavy fuel. Engine specific parameters were investigated by performing measurements of the ship under different operating conditions, including measurements during maneuvering and sailing near the port.

In addition to AVL Boost, AVL Cruise has been used for software simulation of vehicles and engines. Shatrov et al. [66] discussed the features and usage of the AVL Cruise M and showed an example of building a vehicle model. Nagi et al. [67] used AVL-CRUISE for passenger car operation simulation to calculate HC and NOx emission values based on input data, including engine torque, air-fuel ratio and clutch transfer torque. The output matched the experimental data and could be used to simulate SI engine emissions under different vehicle operation parameters and demonstrated its accuracy and reliability. Poojitganont et al. [68] studied the impact of hydrogen fuel on bus fuel efficiency and emissions using AVL Cruise simulated driving parameters. A Mercedes Conecto LF city bus with a diesel engine was simulated and compared with a hydrogen-containing fuel in terms of specific fuel consumption, concluding that hydrogen consumes significantly less fuel than diesel. Yaşar et al. [69] has carried out similar work.

In combination with the AVL Boost and AVL Cruise, Arat et al. [70] [71] carried out experimental simulations of the effects of hydrogen fuel on engine performance and emissions based on the model of a 1.8 L spark-ignition engine and a standard diesel car with a 3.0 L diesel engine, respectively concluding that performance parameters were improved by 3.56% and 4.26% and that emissions were reduced by around 15-30%.

Dhand et al. [72] adopted an integrated approach in a full vehicle model experiment on fuel economy and emissions prediction during the cold start cycle of a vehicle, integrating a cyclic engine model and a cooling circuit model built with AVL Boost and Flowmaster separately, into the vehicle simulation model. AVL Cruise acted as the main model controlling the sequence of implementation and providing data exchange between the other models, thus improving the prediction accuracy of fuel consumption and emissions.

Besides the use of simulation software for modelling engines for emission prediction, there is a certain feasibility of simulation of the after treatment system. Wurzenberger et al. [73] proposed a technology and modelling methodology that combines vehicle, engine and exhaust after treatment system to reduce NOx emissions. Lv et al. [74] proposes a method for modelling the after treatment system based on the AVL CRUISE M for diesel engines, using thermal, pressure and emission parameters for virtual calibration development, building models based on detailed physico-chemical reaction mechanisms and after treatment system models through CRUISE, and improving the accuracy of the models by automatically adjusting the model parameters based on measured data. However Parikh et al. [75] observed biases in the calibration of the model for TWC and analysed them, identifying three biased parameters in the construction of the model, namely the discrepancy in the diffusion rate, the complexity of the objective function to input to the optimiser and the transient conditional accuracy

of the steady-state data. Other than the above software, Athrashalil Phaily et al. and Kuta et al. carried out modelling simulations of the SCR as well, using AVL Fire and Ansys Fluent respectively. The former focusing on the simulation of a single-cylinder diesel engine and the latter on the 3D geometry of the SCR, and accordingly obtained the performance of the SCR as a basis for subsequent optimisation.

The above studies have focused on the use of AVL Cruise/Cruise M and AVL Boost software for vehicle emissions and after treatment system modelling studies, with simulation techniques to validate their effectiveness in tuning vehicle performance and emissions targets, including the effect of hydrogen fuel on fuel economy and emissions, as well as the simulation of after treatment systems. In combination, some studies have aimed at full vehicle modelling experiments, integrating different models to improve accurate predictions of fuel consumption and emissions. However, there are still research gaps, such as the simulation of emissions from a mixture of multiple alternative fuels and gasoline, and the investigation of the synergistic effects of alternative fuels and after treatment systems on engine emission control in the powertrain dimension. Therefore, based on the above foundations, this study proposes a feasible solution for the study of synergies between alternative fuels and emission after treatment systems for emission control of internal combustion engines through the simulation of after treatment system and alternative fuel engine models, which provides valuable information for future research and application in this area.

# 3. METHODOLOGY

## 3.1 Experimental setup and methods

The experimental analysis was carried out on a dedicated engine test rig equipped with a 3-cylinder 1.5 Liter turbocharged GDI engine. The complete schematic of the test setup is shown in Fig. 5, and the main parameters of the engine are shown in Table 3. The engine speed and load were varied and the fuel consumption rate and brake mean effective pressure (BMEP) of the engine under different conditions were recorded for plotting the engine maps. The concentrations of CO, $CO_2$, NOx and THC in the exhaust gases of the engine at different engine speeds and BMEP conditions were measured using FTIR and H-Sense in order to create maps of the engine emissions for engine modelling.

Table 3 Test Engine Specifications

| Number of Cylinders | Compression Ratio | Displacement (L) | Bore (mm) | Stroke (mm) |
|---|---|---|---|---|
| 3 Cylinders | 11：1 | 1.5 L | 84 mm | 90 mm |

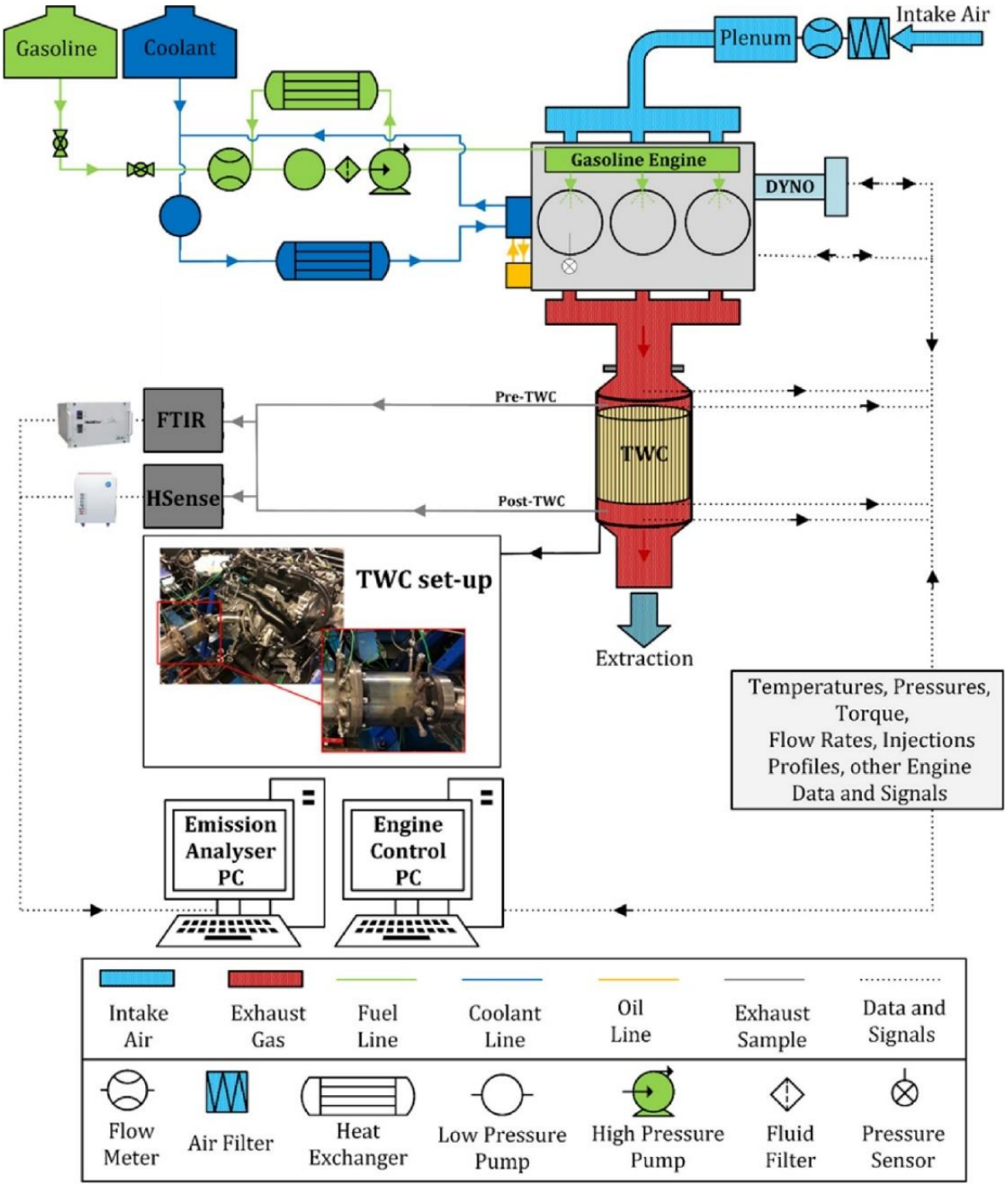


Figure 5 Test set up schematic [76]

## 3.2 Modelling of coupled engine and exhaust after treatment system

### 3.2.1 Model construction

The model was built using AVL cruise M being divided into three main parts. The first part are the engine maps, the concentration profiles of 11 gases including $CO_2$, CO,

NOx, THC at different engine speeds and the mass flow and temperature profiles of the exhaust gas. The second part is the engine, which is built according to the 1.5 L 3-cylinder GDI engine used in the laboratory, and by using the map based engine component. It links the emissions data measured in the laboratory and connects it to the exhaust system. Map based engine outputs the corresponding exhaust gas mass flow and temperature according to the engine speed and the BMEP and simulates the proportion of each component in the exhaust gas to the exhaust system. The third part is the exhaust system and after treatment system, which consists of mass flow boundary, exhaust manifold, restriction and system boundary, and the geometrical parameters are set according to actual laboratory measurements. The after treatment system consists of TWC component and SCR component, catalyst material is cordierite, length is 300 mm, volume is 10 L, and the measurement points are set up before and after the TWC and after the SCR to measure the concentration of emissions. A flange is used to connect to the engine mechanical port as a dynamometer to control the engine torque. The schematic of the model is shown in Figure 6.

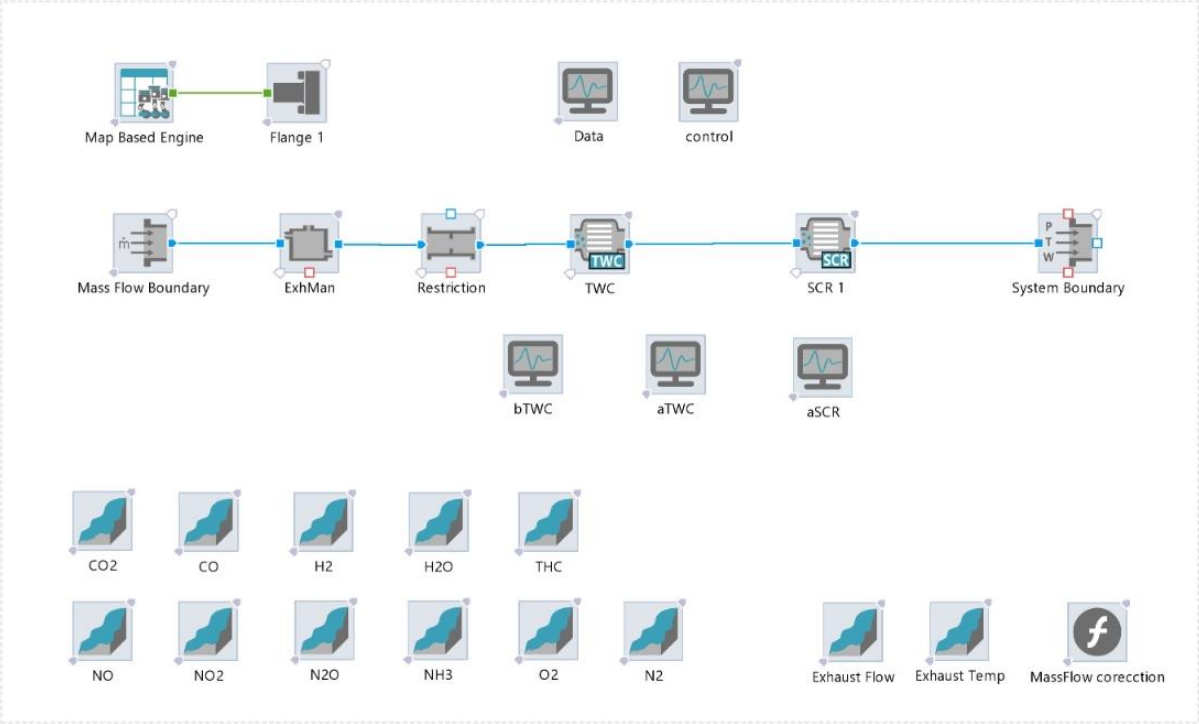


Figure 6 After treatment system model schematic

### 3.2.2 Simulation

According to its working principle, the map based engine outputs the RPM and BMEP under the current working conditions to the RPM-BMEP-concentration maps of each exhaust component, and every map can output the corresponding concentration data to the mass flow boundary, and then enter the exhaust and after treatment system. The map data is derived from experimental data from a laboratory engine.

The engine speed was kept at 2000 rpm, the engine load was kept at 20 Nm and 40 Nm, and the concentration of each component in the exhaust gas was measured at each measurement point for a duration of 400 seconds.

## 3.3 Modelling of alternative fuel engine

### 3.3.1 Model construction

In order to further predict the impact of $H_2$ energy substitution ratios and other zero-carbon fuels on the emissions, the engine is modelled with the cylinder block component of AVL Cruise M. A map based engine modelling approach has not been utilised as there is not available experimental data to build the map based engine model. In contrast to the map based engine, a complete gas circuit containing the system boundary, the intake and exhaust pipelines, and the throttle, which is connected to the cylinder block to form a complete gas cycle, is required, as shown in Figure 7. Since the gas circuit contains combustion chamber elements, only classic species can be chosen as the type of gas composition.

The cylinder block contains two levels of subsystems, consisting of three identical cylinders containing subsystems and are interlinked. Each cylinder block consists of an intake port, an exhaust port and a combustion chamber. In addition, to simulate direct injection, a direct injector is also installed in the cylinder block subsystem and is connected directly to the fuel port of the combustion chamber, and the other end is connected to the fuel tank in the system. The lift curves for the intake and exhaust valves are obtained from laboratory tests rig, and the air ports of valves are connected to intake and exhaust manifolds and combustion chamber.

Engine geometry parameters such as bore, stroke, and compression ratio are entered in the combustion chamber (see Table 3). Combustion and emissions calibration can be undertaken in the manual combustion refinement and manual emissions refinement interfaces to calibrate the emission models for CO, THC, NOx and PN, and set the combustion mode of the combustion chamber to AVL Engineering enhanced gasoline to obtain detailed emissions data. Injection timing and duration, rail pressure, coolant and oil temperature of the engine are connected to a constant component via data bus, the ignition angle is adjusted by connecting to the monitor via data bus. The quantity of fuel injection is converted by a function component and connected to the data bus to be adjusted by the monitor for lambda. A flange is connected to the mechanical port to be used as a dynamometer, which is connected to the data bus to control the engine speed in monitor, and the engine intake is controlled with the throttle to adjust the engine output torque. A NOx sensor is connected to the engine via the data bus to output real-time NOx emissions to the monitor.

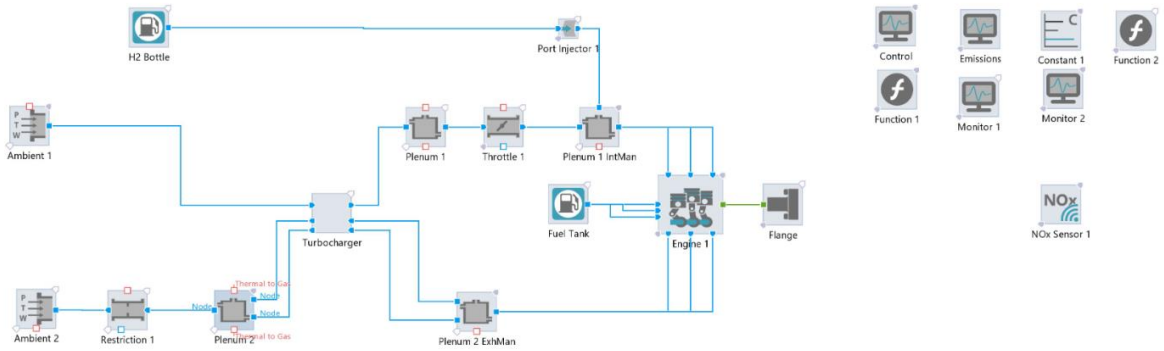


Figure 7 Alternative fuel engine model schematic

The current version of AVL Cruise M software supports a dual fuel definition, so another fuel tank is set up in the system as a $H_2$ tank, which is connected to a third node in the intake manifold via a mass flow connection to allow the injection of hydrogen into the engine intake. A new composition is added to the $H_2$ tank in the gas composition, set to $H_2$+$NH_3$, and the mixing ratio of the two fuels can be set arbitrarily in the fuel specification, or the fuel composition can be added. The mass flow input port of the mass flow connection is connected to the monitor, and the flow rate of the $H_2$ bottle can be controlled in real time during the experiment.

### 3.3.2 Simulation

Five engine conditions, 1500 rpm 15 Nm, 1900 rpm 3 Nm, 2000 rpm 30 Nm, 2100 rpm 15 Nm, 2100 rpm 50 Nm, are selected for simulation, and the engine BMEP and exhaust gas flow under the above conditions are compared with experimental data to verify the reliability of the engine exhaust simulation.

After verifying that the engine model is operating within 5% deviation (engine performance and emissions calibration parameters), the engine model is operated at 2100 rpm, 30 Nm under pure gasoline conditions, and the concentrations of different components in the exhaust gas are measured and compared with experimental data under the same conditions to verify the accuracy of the three exhaust gas prediction models, CO, NOx, and THC. In addition, the map based engine is also run at 2100 rpm, 30 Nm, and the engine exhaust is measured to be compared with the emissions

of alternative fuel engine model running in pure gasoline mode under the same conditions.

The engine model is maintained at 2100 rpm, 30 Nm, a proven operating condition, and the lambda is kept at 1 to exclude the effect of engine air-fuel ratio on exhaust emissions. After the model is running under stable conditions, hydrogen is gradually injected into the intake manifold at various flow rates of 50 g/h, 100 g/h, 200 g/h, 300 g/h, 300 g/h, and 400 g/h to obtain the CO, NOx, and THC concentrations under different hydrogen energy substitution ratios. After $H_2$ flow rate reaches 400 g/h, the fuel composition of $H_2$ bottle is modified by adding $NH_3$ as a fuel blend with ammonia/hydrogen volume ratio of 5:1, which is injected into the intake manifold at a mass flow rate of 400 g/h, to obtain the CO, NOx, and THC concentrations in the exhaust gas under this condition.

# 4. RESULTS AND DISCUSSION

## 4.1 Simulation of coupled engine and exhaust after treatment system working with gasoline fuel

### 4.1.1 CO and $CO_2$ emissions

For this section a map-based engine has been used in the model, therefore the model already included experimental values in the calibration and validation process as explain in the methodology section of the thesis. Figures 8 and 9 show the simulated CO and $CO_2$ concentration curves before and after the TWC at 2000 rpm, 20 Nm and 40 Nm. During the time period of 0-400 seconds, the catalyst temperature is gradually increased from the initial temperature to the working temperature, so this stage is regarded as the warm-up of the catalyst. It should be clarified that there are no fluctuation of CO and $CO_2$ engine output concentration during the catalyst warm-up stage, as the engine is maintained at steady state engine operation condition of 20 Nm. After the TWC treatment of the exhaust gas, more than 99.99% of the CO is oxidised into $CO_2$. The engine load is increased to 40 Nm, leading to an approximately 4% increase in the CO concentration. Similarly, CO is completely oxidised to $CO_2$ after TWC, causing an increase in the concentration of the latter. In both cases the TWC light off temperature was reached.

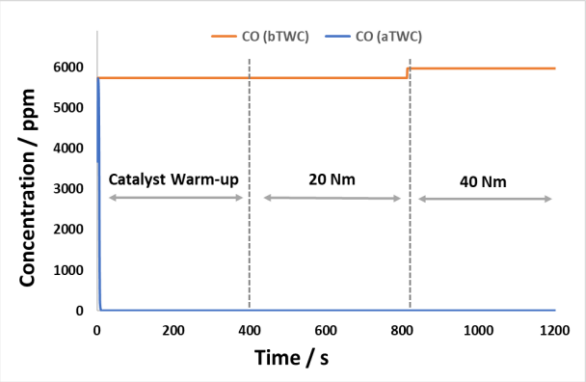


Figure 8 CO concentration

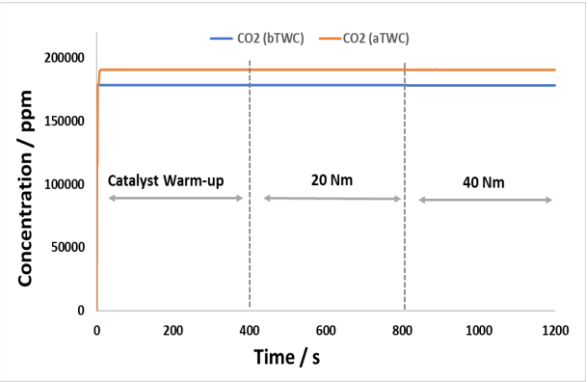


Figure 9 $CO_2$ concentration

### 4.1.2 NOx emissions

Fig. 10 and Fig. 11 show the NO and $NO_2$ concentration curves before and after TWC at 2000 rpm 20 Nm and 40 Nm respectively. On warm-up TWC cannot have an effect on NO for a very short period of time. It is due to the catalyst temperature not reaching the operating temperature range during the warm-up stage. After fluctuation the concentration of NO after TWC increases slowly and remains stable in the period of 400 to 800s with the conversion of NO by TWC being 87.32%. While the engine load is raised to 40 Nm, the NO concentration significantly increases to 2100 ppm, but the TWC can still maintain an 85.58% conversion rate. $NO_2$ concentration is always kept at a very low level under pure gasoline conditions. The increase of $NO_2$ emissions after TWC caused by the introduction of alternative fuels (if any) can be further treated by other deNOx catalysts (e.g. $NH_3$-SCR catalyst, $H_2$-SCR catalyst, etc.).

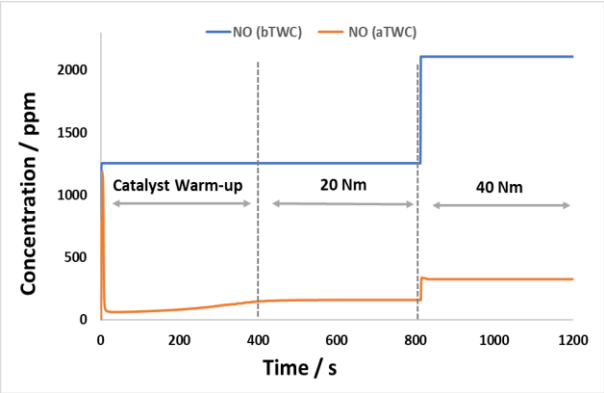


Figure 10 NO concentration

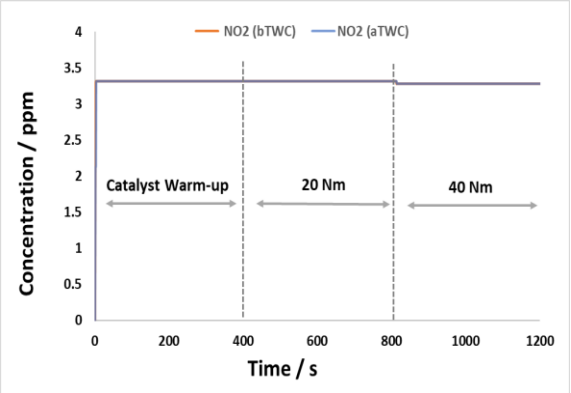


Figure 11 $NO_2$ concentration

### 4.1.3 THC emissions

Figure 12 shows the hydrocarbon (THC) concentration curves before and after TWC at 2000 rpm 20 Nm and 40 Nm. TWC rapidly converts incompletely burnt THC into non-toxic and non-hazardous $CO_2$ after warm-up, which is one of the reasons for the increase of $CO_2$ content in the exhaust gas after TWC treated. After increasing load to 40 Nm, THC in engine exhaust gas was reduced by about 3.5%, and conversion efficiency of TWC remained above 99.99%.

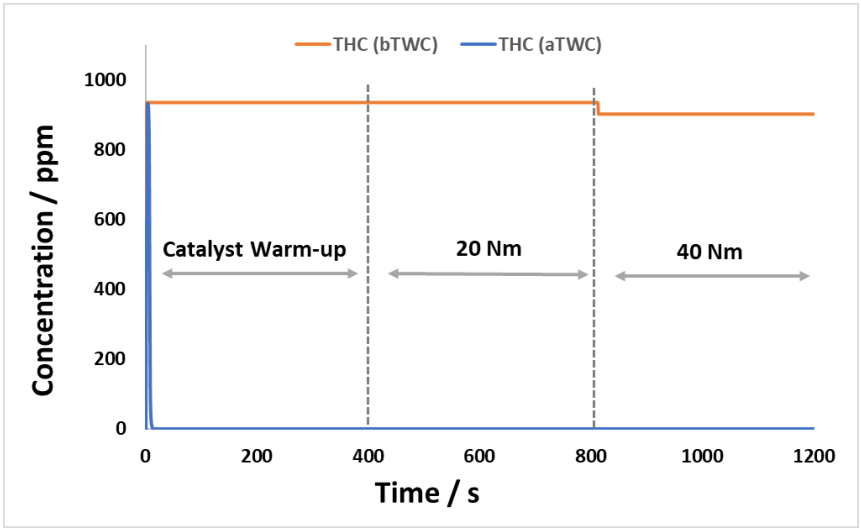


Figure 12 THC concentration

In conclusion, a coupled engine and TWC working with gasoline fuel has successfully modelled showing that the TWC has a high conversion efficiency for CO, NO and THC, converting them into non-toxic and non-hazardous $N_2$, $H_2O$ and $CO_2$ when the engine is operated at stoichiometric conditions. However, the performance of catalysts will be affected by the type of fuel, such as zero carbon fuels, which will be presented in next section. It has to be clarified that the catalyst performance is also affected by engine operation (lambda), the catalyst's geometrical parameters, long-term operation at high temperatures, which are out of scope of this thesis.

## 4.2 Simulation of alternative fuel engine

### 4.2.1 Calibration and validation

It has to be noted that in this case an engine map based model can not been obtained to predicate emissions from high energy substitute ratios of alternative fuels as there is not sufficient experimental data available. Therefore, in this case the model needs to be independently calibrated and validated as explained in the methodology section. The model calibration was carried out under pure gasoline conditions and the engine emission model was calibrated after assuring that the geometrical parameters of the engine model were exactly matched with the engine used in the laboratory rig. Since the function to calibrate the three emission formation models is integrated in AVL Cruise M, only the comparison of experimental data with simulation data was required. Settings for CO emission rich correction, CO emission offset, NOx emission correction,

and THC emission correction were applied to calibrate the model emissions, and then afterwards a validation was carried out.

Figure 13 shows the experimental data and simulation data of BMEP and exhaust mass flow at five operating points: 15 Nm at 1500 rpm, 3 Nm at 1900 rpm, 30 Nm at 2000 rpm, 15 Nm at 2100 rpm, and 50 Nm at 2100 rpm. The maximum value of error calculated is 3.45% $(Error = \frac{Simulation\ Data - Experimental\ Data}{Experimental\ Data} \times 100\%)$. The test condition of 2100 rpm 30 Nm is selected and the three emission formation models, CO model, NOx model and THC model in AVL Engineering enhanced gasoline combustion model of the engine are measured under this condition. The comparison of the results with the experimental data under this condition is shown in Fig. 14. The maximum deviation of THC is approximately 1.77%. It is verified that this engine simulation model can be used for simulation experiments within an error range of 5%.

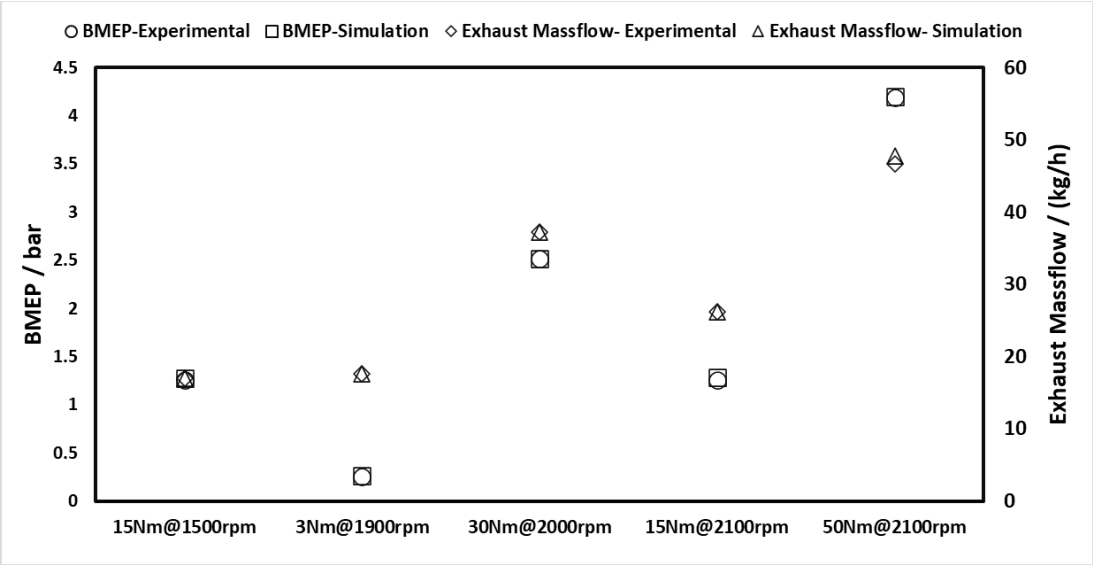


Figure 13 Validation of BMEP and exhaust mass flow

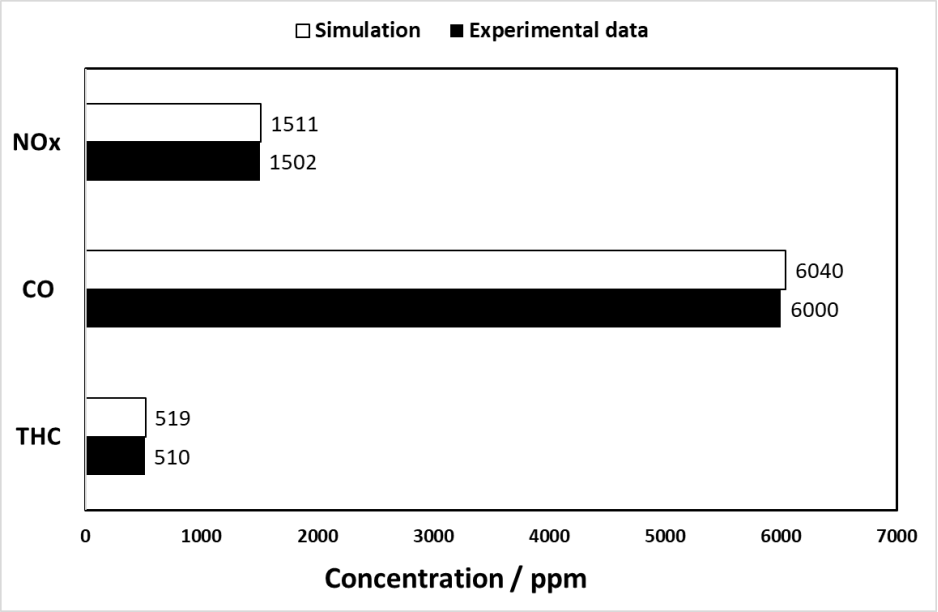


Figure 14 Validation of emissions

The THC, CO, and NOx concentrations measured at 2100 rpm and 30 Nm for the map based engine and the cylinder block in pure petrol mode are shown in Fig. 15, and the deviation of the concentration produced by the two models is within 1%, which verifies the accuracy of the models. The data from the map based engine model is selected as the baseline of pure gasoline condition for the comparison in the subsequent simulation.

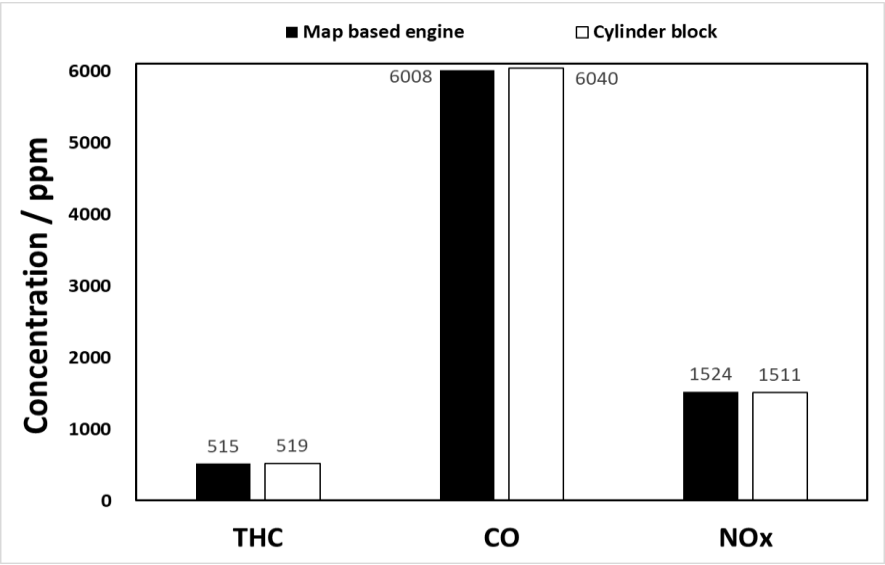


Figure 15 Comparison between two models at 2100 rpm 30 Nm

### 4.2.2 Simulation results of emissions

Figure 16 shows the variation of CO, NOx, THC content in exhaust gas of this engine model at 2100 rpm 30 Nm load with increasing $H_2$ mass flow injected into the intake manifold, maintaining the engine lambda at 1 throughout the test. Hydrogen is a zero carbon fuel, which also has a higher combustion heating value, higher combustion speed and higher adiabatic flame temperature than gasoline fuel, thus improving the combustion process and combustion temperature. As a result, the engine output CO concentration is reduced by one third and THC are also slightly reduced. On the other hand, the higher $H_2$ combustion temperature results in an increase of NOx emissions. When the hydrogen flow rate continues to be increased, for instance to 100 g/h, the original ignition timing is no longer optimal. Hence the incomplete combustion caused by inappropriate ignition timing results in an increase of about 45 ppm in CO concentration instead of a decrease, and a small percentage rise in NOx. Therefore, the subsequent increase in the hydrogen concentration is accompanied by an advance of 1 to 2 degrees in ignition timing. This also shows that the synergistic optimisation of ignition timing and hydrogen energy substitution ratio is significant for emission control. After further increasing the flow rate of $H_2$ injection and optimising the ignition timing, the NOx emission continued to increase to a high level of 2739 ppm after reaching a hydrogen flow rate of 400 g/h, and then CO concentration was reduced to less than half of the pure gasoline condition, facilitated by hydrogen. Throughout the process of

increasing $H_2$ flow, THC levels continuously decrease, but at the same time, they are also dramatically affected by ignition timing.

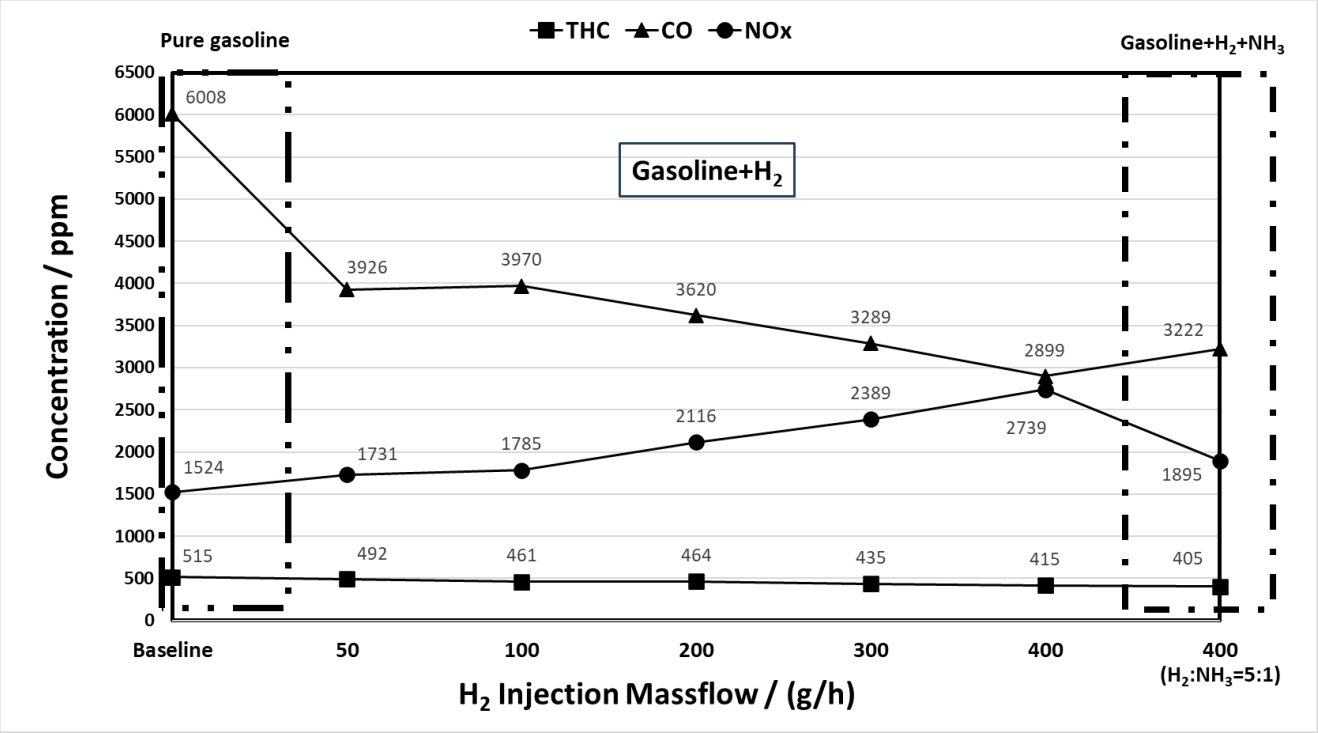


Figure 16 Emission simulation

When introducing ammonia-hydrogen blended fuel injected into intake manifold at a flow rate of 400 g/h, under the same conditions of 2100 rpm 30 Nm and lambda=1, the higher combustion temperature due to the higher heating value of $H_2$ was partially offset by a higher combustion resistance value of $NH_3$, which suppressed the formation of NOx; compared to 400 g/h pure hydrogen injection, NOx concentration was reduced by 31%. It helps to reduce the burden of NOx catalytic reduction in after treatment system. However, the reduction in combustion temperature also leads to a slight increase in CO concentration compared to the 400 g/h pure hydrogen test, but the overall CO emission is reduced by about 46% relative to pure gasoline combustion,

and according to the results of after treatment system simulation experiments, TWC can convert most of the CO into $CO_2$ emission within this value range. A small reduction in the concentration of THC is achieved by optimising the engine ignition timing with the introduction of $NH_3$.

In summary, ammonia and hydrogen as two types of zero-carbon fuels with different characteristics, $H_2$ has a relatively high flame speed and thermal value, but its energy density is low, and there is some hazard in the storage and transport; $NH_3$ has a high energy density, it can reach 13.6 $GJ/m^3$ [77], which is three times as high as that of hydrogen, but its combustion resistance is larger, so the performance in the case of combustion assisted by $H_2$, or others, as a combustion enhancer is better. Therefore, by blending these two zero carbon fuels, the combustion characteristics could be complementary with each other, by replacing carbon-based fuels with catalytic reactions in the after treatment system, internal combustion engine carbon reduction and NOx reduction could be achieved at the same time.

# 5. CONCLUSIONS AND FURTHER WORK

## Conclusions

1. A coupled map based engine and exhaust aftertreatment model has been built in AVL Cruise with the input of engine output emissions experimental data. The TWC model is able to reproduce the expected catalytic conversion trends in terms of CO, THC and NOx conversion. It also proves the necessity of introducing zero-carbon fuels for emission control of internal combustion engine, especially for decarbonization.

2. An engine model able to simulate engine operation under zero carbon fuels has been built in AVL Cruise M. It is verified that the model is able to carry out simulation tests within an error range of less than 5% and predict the impact of alternative fuel with high energy substitution ratios on engine emissions.

3. Hydrogen and ammonia-hydrogen blended fuels are introduced in the alternative fuel engine emission simulation model. Changes in emissions such as CO, NOx, and THC under different hydrogen energy substitution ratios are simulated, and the effect of introducing $NH_3$ is studied. The results show that zero-carbon fuels can effectively achieve carbon reduction in internal combustion engines, and the ammonia-hydrogen blended fuels can, in a certain extent, achieve complementary combustion characteristics, and better emission control can be achieved by optimising the ignition timing and synergising with the after treatment system.

## Further Work

Due to the limitation of the emission formation model of AVL Cruise M software, this study only simulated after treatment system and alternative fuel engine separately. And as there is not sufficient experimental data for coupled map based engine and exhaust after treatment model running under other lambda conditions, SCR catalyst dose not perform sufficiently under stoichiometric conditions to verify its NOx after treatment capability. In future studies, further optimisation of this model can be carried out and linked to external combustion model to obtain complete engine exhaust composition which can be imported into the after treatment model to explore a direct and comprehensive impact of after treatment system on combustion products of alternative fuels.

# References


[1]F. Zhao, Z. Wang, D. Wang, F. Han, Y. Ji, and W. Cai, ‘Top level design and evaluation of advanced low/zero carbon fuel ships power technology’, *Energy Reports*, vol. 8, pp. 336–344, Nov. 2022, doi: 10.1016/j.egyr.2022.10.143.

[2]S. Kumar *et al.*, ‘LNG: An eco-friendly cryogenic fuel for sustainable development’, *Applied Energy*, vol. 88, no. 12, pp. 4264–4273, Dec. 2011, doi: 10.1016/j.apenergy.2011.06.035.

[3]M. Jayakumar *et al.*, ‘A comprehensive outlook on topical processing methods for biofuel production and its thermal applications: Current advances, sustainability and challenges’, *Fuel*, vol. 349, p. 128690, Oct. 2023, doi: 10.1016/j.fuel.2023.128690.

[4]Omer Berkehan Inal, Burak Zincir, and Caglar Dere, ‘Hydrogen as Maritime Transportation Fuel: A Pathway for Decarbonization’, [Online]. Available: https://doi.org/10.1007/978-981-16-8344-2_4

[5]H. L. Yip *et al.*, ‘A Review of Hydrogen Direct Injection for Internal Combustion Engines: Towards Carbon-Free Combustion’, *Applied Sciences*, vol. 9, no. 22, p. 4842, Nov. 2019, doi: 10.3390/app9224842.

[6]Y. Wang *et al.*, ‘A review of low and zero carbon fuel technologies: Achieving ship carbon reduction targets’, *Sustainable Energy Technologies and Assessments*, vol. 54, p. 102762, Dec. 2022, doi: 10.1016/j.seta.2022.102762.

[7]C. Zamfirescu and I. Dincer, ‘Using ammonia as a sustainable fuel’, *Journal of Power Sources*, vol. 185, no. 1, pp. 459–465, Oct. 2008, doi: 10.1016/j.jpowsour.2008.02.097.

[8]H. Kobayashi, A. Hayakawa, K. D. K. A. Somarathne, and E. C. Okafor, ‘Science and technology of ammonia combustion’, *Proceedings of the Combustion Institute*, vol. 37, no. 1, pp. 109–133, 2019, doi: 10.1016/j.proci.2018.09.029.

[9]W. Wang, J. M. Herreros, A. Tsolakis, and A. P. E. York, ‘Ammonia as hydrogen carrier for transportation; investigation of the ammonia exhaust gas fuel reforming’, *International Journal of Hydrogen Energy*, vol. 38, no. 23, pp. 9907–9917, Aug. 2013, doi: 10.1016/j.ijhydene.2013.05.144.

[10] E. Nadimi, G. Przybyła, M. T. Lewandowski, and W. Adamczyk, ‘Effects of ammonia on combustion, emissions, and performance of the ammonia/diesel dual-fuel compression ignition engine’, *Journal of the Energy Institute*, vol. 107, p. 101158, Apr. 2023, doi: 10.1016/j.joei.2022.101158.

[11] J. Zhu, D. Zhou, W. Yang, Y. Qian, Y. Mao, and X. Lu, ‘Investigation on the potential of using carbon-free ammonia in large two-stroke marine engines by dual-fuel combustion strategy’, *Energy*, vol. 263, p. 125748, Jan. 2023, doi: 10.1016/j.energy.2022.125748.
[12] T. Li *et al.*, ‘A comparison between low- and high-pressure injection dual-fuel modes of diesel-pilot-ignition ammonia combustion engines’, *Journal of the Energy Institute*, vol. 102, pp. 362–373, Jun. 2022, doi: 10.1016/j.joei.2022.04.009.
[13] L. Liu, J. Wu, H. Liu, Y. Wu, and Y. Wang, ‘Study on marine engine combustion and emissions characteristics under multi-parameter coupling of ammonia-diesel stratified injection mode’, *International Journal of Hydrogen Energy*, vol. 48, no. 26, pp. 9881–9894, Mar. 2023, doi: 10.1016/j.ijhydene.2022.12.065.
[14] L. Liu, F. Tan, Z. Wu, Y. Wang, and H. Liu, ‘Comparison of the combustion and emission characteristics of NH3/NH4NO2 and NH3/H2 in a two-stroke low speed marine engine’, *International Journal of Hydrogen Energy*, vol. 47, no. 40, pp. 17778–17787, May 2022, doi: 10.1016/j.ijhydene.2022.03.239.
[15] A. A. Boretti, ‘Novel heavy duty engine concept for operation dual fuel H2–NH3’, *International Journal of Hydrogen Energy*, vol. 37, no. 9, pp. 7869–7876, May 2012, doi: 10.1016/j.ijhydene.2012.01.091.
[16] W. Wang, J. M. Herreros, A. Tsolakis, and A. P. E. York, ‘Reducing CO2 footprint through synergies in carbon free energy vectors and low carbon fuels’, *Energy*, vol. 112, pp. 976–983, Oct. 2016, doi: 10.1016/j.energy.2016.07.010.
[17] J. Li, R. Zhang, J. Pan, H. Wei, G. Shu, and L. Chen, ‘Ammonia and hydrogen blending effects on combustion stabilities in optical SI engines’, *Energy Conversion and Management*, vol. 280, p. 116827, Mar. 2023, doi: 10.1016/j.enconman.2023.116827.
[18] C. Hong *et al.*, ‘An experimental study of various load control strategies for an ammonia/hydrogen dual-fuel engine with the Miller cycle’, *Fuel Processing Technology*, vol. 247, p. 107780, Aug. 2023, doi: 10.1016/j.fuproc.2023.107780.
[19] C. S. Mørch, A. Bjerre, M. P. Gøttrup, S. C. Sorenson, and J. Schramm, ‘Ammonia/hydrogen mixtures in an SI-engine: Engine performance and analysis of a proposed fuel system’, *Fuel*, vol. 90, no. 2, pp. 854–864, Feb. 2011, doi: 10.1016/j.fuel.2010.09.042.
[20] C. Lhuillier, P. Brequigny, F. Contino, and C. Mounaïm-Rousselle, ‘EXPERIMENTAL STUDY ON NH3/H2/AIR COMBUSTION IN SPARK-IGNITION ENGINE CONDITIONS’.

[21] G. Xin, C. Ji, S. Wang, H. Meng, K. Chang, and J. Yang, ‘Effect of ammonia addition on combustion and emission characteristics of hydrogen-fueled engine under lean-burn condition’, *International Journal of Hydrogen Energy*, vol. 47, no. 16, pp. 9762–9774, Feb. 2022, doi: 10.1016/j.ijhydene.2022.01.027.

[22] M. H. Dinesh, J. K. Pandey, and G. N. Kumar, ‘Study of performance, combustion, and NOx emission behavior of an SI engine fuelled with ammonia/hydrogen blends at various compression ratio’, *International Journal of Hydrogen Energy*, vol. 47, no. 60, pp. 25391–25403, Jul. 2022, doi: 10.1016/j.ijhydene.2022.05.287.

[23] G. Sathish Sharma, M. Sugavaneswaran, and R. Prakash, ‘Chapter 8 - NOx reduction in IC engines through after treatment catalytic converter’, in *NOx Emission Control Technologies in Stationary and Automotive Internal Combustion Engines*, B. Ashok, Ed., Elsevier, 2022, pp. 223–253. doi: 10.1016/B978-0-12-823955-1.00008-5.

[24] V. Praveena and M. L. J. Martin, ‘A review on various after treatment techniques to reduce NOx emissions in a CI engine’, *Journal of the Energy Institute*, vol. 91, no. 5, pp. 704–720, Oct. 2018, doi: 10.1016/j.joei.2017.05.010.

[25] G. G. Naik and H. M. Dharmadhikari, ‘Methods for reducing NOx and PM emissions in compression ignition engine: A review’, *Materials Today: Proceedings*, vol. 72, pp. 1406–1412, 2023, doi: 10.1016/j.matpr.2022.09.339.

[26] S. Feng *et al.*, ‘An overview of the deactivation mechanism and modification methods of the SCR catalysts for denitration from marine engine exhaust’, *Journal of Environmental Management*, vol. 317, p. 115457, Sep. 2022, doi: 10.1016/j.jenvman.2022.115457.

[27] T. Andana, K. G. Rappé, F. Gao, J. Szanyi, X. Pereira-Hernandez, and Y. Wang, ‘Recent advances in hybrid metal oxide–zeolite catalysts for low-temperature selective catalytic reduction of NOx by ammonia’, *Applied Catalysis B: Environmental*, vol. 291, p. 120054, Aug. 2021, doi: 10.1016/j.apcatb.2021.120054.

[28] R. Chen, S. Peng, Y. Wang, X. Qi, and Z. Liu, ‘Selective catalytic reduction of NO with NH3 over core-shell Ce@W catalyst’, *Journal of Rare Earths*, p. S1002072123000054, Jan. 2023, doi: 10.1016/j.jre.2023.01.005.

[29] Y. Wei *et al.*, ‘Modification of Mn-Fe mixed oxide catalysts for low-temperature NH3-SCR of NO from marine diesel exhausts’, *Journal of Environmental Chemical Engineering*, vol. 10, no. 3, p. 107772, Jun. 2022, doi: 10.1016/j.jece.2022.107772.

[30] W. Liu *et al.*, ‘Commercial SCR catalyst modified with different noble metals (Ag, Pt, Pd) to efficiently remove slip ammonia and NOx in the flue gas’, *Journal of the Taiwan Institute of Chemical Engineers*, vol. 138, p. 104472, Sep. 2022, doi: 10.1016/j.jtice.2022.104472.
[31] X. Li *et al.*, ‘Acid treatment of ZrO2-supported CeO2 catalysts for NH3-SCR of NO: Influence on surface acidity and reaction mechanism’, *Journal of the Taiwan Institute of Chemical Engineers*, vol. 132, p. 104144, Mar. 2022, doi: 10.1016/j.jtice.2021.11.011.
[32] W. Wang, J. M. Herreros, A. Tsolakis, and A. P. E. York, ‘Increased NO2 concentration in the diesel engine exhaust for improved Ag/Al2O3 catalyst NH3-SCR activity’, *Chemical Engineering Journal*, vol. 270, pp. 582–589, Jun. 2015, doi: 10.1016/j.cej.2015.02.067.
[33] D. E. Doronkin *et al.*, ‘Study of the “Fast SCR”-like mechanism of H2-assisted SCR of NOx with ammonia over Ag/Al2O3’, *Applied Catalysis B: Environmental*, vol. 113–114, pp. 228–236, Feb. 2012, doi: 10.1016/j.apcatb.2011.11.042.
[34] D. E. Doronkin, T. S. Khan, T. Bligaard, S. Fogel, P. Gabrielsson, and S. Dahl, ‘Sulfur poisoning and regeneration of the Ag/γ-Al2O3 catalyst for H2-assisted SCR of NOx by ammonia’, *Applied Catalysis B: Environmental*, vol. 117–118, pp. 49–58, May 2012, doi: 10.1016/j.apcatb.2012.01.002.
[35] D. E. Doronkin, S. Fogel, P. Gabrielsson, J.-D. Grunwaldt, and S. Dahl, ‘Ti and Si doping as a way to increase low temperature activity of sulfated Ag/Al2O3 in H2-assisted NH3-SCR of NOx’, *Applied Catalysis B: Environmental*, vol. 148–149, pp. 62–69, Apr. 2014, doi: 10.1016/j.apcatb.2013.10.040.
[36] A. Wang *et al.*, ‘NH3-SCR on Cu, Fe and Cu + Fe exchanged beta and SSZ-13 catalysts: Hydrothermal aging and propylene poisoning effects’, *Catalysis Today*, vol. 320, pp. 91–99, Jan. 2019, doi: 10.1016/j.cattod.2017.09.061.
[37] C. N. Costa, P. G. Savva, J. L. G. Fierro, and A. M. Efstathiou, ‘Industrial H2-SCR of NO on a novel Pt/MgO–CeO2 catalyst’, *Applied Catalysis B: Environmental*, vol. 75, no. 3–4, pp. 147–156, Sep. 2007, doi: 10.1016/j.apcatb.2007.04.018.
[38] Y. Guan, Y. Liu, Q. Lv, B. Wang, and D. Che, ‘Review on the selective catalytic reduction of NO with H2 by using novel catalysts’, *Journal of Environmental Chemical Engineering*, vol. 9, no. 6, p. 106770, Dec. 2021, doi: 10.1016/j.jece.2021.106770.
[39] S. S. Kim and S. C. Hong, ‘Relationship between the surface characteristics of Pt catalyst and catalytic performance on the H2

SCR’, *Journal of Industrial and Engineering Chemistry*, vol. 16, no. 6, pp. 992–996, Nov. 2010, doi: 10.1016/j.jiec.2010.07.022.
[40] K. Duan, Z. Liu, J. Li, L. Yuan, H. Hu, and S. I. Woo, ‘Novel Pd-Au/TiO2 catalyst for the selective catalytic reduction of NOx by H2’, *Catalysis Communications*, vol. 57, pp. 19–22, Dec. 2014, doi: 10.1016/j.catcom.2014.07.033.
[41] Z. Savva, K. C. Petallidou, C. M. Damaskinos, G. G. Olympiou, V. N. Stathopoulos, and A. M. Efstathiou, ‘H2-SCR of NOx on low-SSA CeO2-supported Pd: The effect of Pd particle size’, *Applied Catalysis A: General*, vol. 615, p. 118062, Apr. 2021, doi: 10.1016/j.apcata.2021.118062.
[42] C. Zhang, Y. Gao, Q. Yan, and Q. Wang, ‘Fundamental investigation on layered double hydroxides derived mixed metal oxides for selective catalytic reduction of NOx by H2’, *Catalysis Today*, vol. 355, pp. 450–457, Sep. 2020, doi: 10.1016/j.cattod.2019.07.006.
[43] G. C. Mondragón Rodríguez and B. Saruhan, ‘Effect of Fe/Co-ratio on the phase composition of Pd-integrated perovskites and its H2-SCR of NOx performance’, *Applied Catalysis B: Environmental*, vol. 93, no. 3–4, pp. 304–313, Jan. 2010, doi: 10.1016/j.apcatb.2009.10.004.
[44] V. K. Patel and S. Sharma, ‘Effect of oxide supports on palladium based catalysts for NO reduction by H2-SCR’, *Catalysis Today*, vol. 375, pp. 591–600, Sep. 2021, doi: 10.1016/j.cattod.2020.04.006.
[45] C. N. Costa and A. M. Efstathiou, ‘Low-temperature H2-SCR of NO on a novel Pt/MgO-CeO2 catalyst’, *Applied Catalysis B: Environmental*, vol. 72, no. 3–4, pp. 240–252, Mar. 2007, doi: 10.1016/j.apcatb.2006.11.010.
[46] S. Yang, X. Wang, W. Chu, Z. Song, and S. Zhao, ‘An investigation of the surface intermediates of H2-SCR of NOx over Pt/H-FER’, *Applied Catalysis B: Environmental*, vol. 107, no. 3–4, pp. 380–385, Sep. 2011, doi: 10.1016/j.apcatb.2011.08.001.
[47] X. Zhang, X. Wang, X. Zhao, Y. Xu, Y. Liu, and Q. Yu, ‘Promotion effect of tungsten on the activity of Pt/HZSM-5 for H2-SCR’, *Chemical Engineering Journal*, vol. 260, pp. 419–426, Jan. 2015, doi: 10.1016/j.cej.2014.09.030.
[48] L. Cao, Q. Wang, and J. Yang, ‘Ultrafine Pt particles directed by polyvinylpyrrolidone on zeolite beta as an efficient low-temperature H2-SCR catalyst’, *Journal of Environmental Chemical Engineering*, vol. 8, no. 1, p. 103631, Feb. 2020, doi: 10.1016/j.jece.2019.103631.
[49] L. Li, P. Wu, Q. Yu, G. Wu, and N. Guan, ‘Low temperature H2-SCR over platinum catalysts supported on Ti-containing MCM-41’, *Applied*

*Catalysis B: Environmental*, vol. 94, no. 3–4, pp. 254–262, Feb. 2010, doi: 10.1016/j.apcatb.2009.11.016.

[50] Y. Liu, M. Tursun, H. Yu, and X. Wang, 'Surface property and activity of Pt/Nb2O5-ZrO2 for selective catalytic reduction of NO by H2', *Molecular Catalysis*, vol. 464, pp. 22–28, Feb. 2019, doi: 10.1016/j.mcat.2018.12.015.

[51] X. Wang, X. Wang, H. Yu, and X. Wang, 'The functions of Pt located at different positions of HZSM-5 in H2-SCR', *Chemical Engineering Journal*, vol. 355, pp. 470–477, Jan. 2019, doi: 10.1016/j.cej.2018.07.207.

[52] Q. Yu, M. Richter, L. Li, F. Kong, G. Wu, and N. Guan, 'The promotional effect of Cr on catalytic activity of Pt/ZSM-35 for H2-SCR in excess oxygen', *Catalysis Communications*, vol. 11, no. 11, pp. 955–959, Jun. 2010, doi: 10.1016/j.catcom.2010.03.021.

[53] X. Zhao, X. Zhang, Y. Xu, Y. Liu, X. Wang, and Q. Yu, 'The effect of H2O on the H2-SCR of NOx over Pt/HZSM-5', *Journal of Molecular Catalysis A: Chemical*, vol. 400, pp. 147–153, May 2015, doi: 10.1016/j.molcata.2015.02.013.

[54] Y. Zhang, S. Xu, Y. Wang, and Z. Liu, 'Selective catalytic reduction of NOx by H2 over Na modified Pd/TiO2 catalyst', *International Journal of Hydrogen Energy*, p. S0360319923001441, Jan. 2023, doi: 10.1016/j.ijhydene.2023.01.099.

[55] G. Jong Kim, J. Hun Shin, S. Bin Kim, and S. Chang Hong, 'The role of Pt valence state and La doping on titanium supported Pt-La/TiO2 catalyst for selective catalytic reduction with H2', *Applied Surface Science*, vol. 608, p. 155040, Jan. 2023, doi: 10.1016/j.apsusc.2022.155040.

[56] Z. Hu, X. Yong, D. Li, and R. T. Yang, 'Synergism between palladium and nickel on Pd-Ni/TiO2 for H2-SCR: A transient DRIFTS study', *Journal of Catalysis*, vol. 381, pp. 204–214, Jan. 2020, doi: 10.1016/j.jcat.2019.11.006.

[57] S. Tamm, N. Vallim, M. Skoglundh, and L. Olsson, 'The influence of hydrogen on the stability of nitrates during H2-assisted SCR over Ag/Al2O3 catalysts – A DRIFT study', *Journal of Catalysis*, vol. 307, pp. 153–161, Nov. 2013, doi: 10.1016/j.jcat.2013.07.003.

[58] Y. Luo, X. Wang, Q. Qian, and Q. Chen, 'Studies on B sites in Fe-doped LaNiO 3 perovskite for SCR of NO x with H 2', *International Journal of Hydrogen Energy*, vol. 39, no. 28, pp. 15836–15843, Sep. 2014, doi: 10.1016/j.ijhydene.2014.07.135.

[59] S. Fogel and P. Gabrielsson, 'H2-assisted NH3-SCR over Ag/Al2O3: An engine-bench study', *Applied Catalysis B: Environmental*, vol. 158–159, pp. 1–10, Oct. 2014, doi: 10.1016/j.apcatb.2014.03.040.

[60] P. Xiang *et al.*, 'Experimental investigation on gas emission characteristics of ammonia/diesel dual-fuel engine equipped with DOC + SCR aftertreatment', *Fuel*, vol. 359, p. 130496, Mar. 2024, doi: 10.1016/j.fuel.2023.130496.

[61] P. Srinivasan and K. U. M, 'Performance Fuel Economy and $CO_2$ Prediction of a Vehicle using AVL Cruise Simulation Techniques', SAE International, Warrendale, PA, SAE Technical Paper 2009-01–1862, Jun. 2009. doi: 10.4271/2009-01-1862.

[62] J. Wheeler *et al.*, 'Design of a 4-Cylinder GTDI Engine with Part-Load HCCI Capability', *SAE Int. J. Engines*, vol. 6, no. 1, pp. 184–196, Apr. 2013, doi: 10.4271/2013-01-0287.

[63] A. F. Pacheco, M. E. S. Martins, and H. Zhao, 'New European Drive Cycle (NEDC) simulation of a passenger car with a HCCI engine: Emissions and fuel consumption results', *Fuel*, vol. 111, pp. 733–739, Sep. 2013, doi: 10.1016/j.fuel.2013.03.060.

[64] F. Salek, M. Babaie, A. Shakeri, S. V. Hosseini, T. Bodisco, and A. Zare, 'Numerical Study of Engine Performance and Emissions for Port Injection of Ammonia into a Gasoline\Ethanol Dual-Fuel Spark Ignition Engine', *Applied Sciences*, vol. 11, no. 4, p. 1441, Feb. 2021, doi: 10.3390/app11041441.

[65] T. C. Van *et al.*, 'Numerical Simulation of Performance and Exhaust Emissions of a Marine Main Engine Using Heavy Fuel Oil during the whole Voyage'.

[66] M. G. Shatrov, A. Yu. Dunin, A. L. Yakovenko, A. S. Stryapunin, and L. N. Golubkov, 'Application of the AVL CRUISE M Software Package for Modeling the Operation of an Engine as Part of a Vehicle', in *2023 Systems of Signals Generating and Processing in the Field of on Board Communications*, Mar. 2023, pp. 1–4. doi: 10.1109/IEEECONF56737.2023.10092096.

[67] M. Nagi, 'SIMULATION OF A PASSENGER CAR PERFORMANCE AND EMISSIONS USING THE AVL-CRUISE SOFTWARE'.

[68] T. Poojitganont, O. Antoshkiv, B. Watjatrakul, and H. P. Berg, 'Efficiency and Emission Simulations of Hydrogen-Fuel City Buses', *IOP Conf. Ser.: Mater. Sci. Eng.*, vol. 886, no. 1, p. 012025, Jul. 2020, doi: 10.1088/1757-899X/886/1/012025.

[69] H. Yaşar and G. Canbolat, 'Fuel Consumption, Exhaust Emission and Vehicle Performance Simulations of a Series-Hybrid Electric Non-Automotive Vehicle', *5th International Symposium on Innovative*

*Technologies in Engineering and Science 29-30 September 2017 (ISITES2017 Baku - Azerbaijan)*, Sep. 2017, Accessed: Jun. 29, 2023. [Online]. Available: https://isites.info/PastConferences/ISITES2017/ISITES2017/Allpapers/A11-ISITES2017ID281.htm

[70] H. T. Arat, 'Alternative fuelled hybrid electric vehicle (AF-HEV) with hydrogen enriched internal combustion engine', *International Journal of Hydrogen Energy*, vol. 44, no. 34, pp. 19005–19016, Jul. 2019, doi: 10.1016/j.ijhydene.2018.12.219.

[71] H. T. Arat, 'Simulation of diesel hybrid electric vehicle containing hydrogen enriched CI engine', *International Journal of Hydrogen Energy*, vol. 44, no. 20, pp. 10139–10146, Apr. 2019, doi: 10.1016/j.ijhydene.2018.10.004.

[72] A. Dhand, T. Cimen, and B. Cho, *FULL VEHICLE MODELLING FOR COLD START CYCLE FUEL ECONOMY AND EMISSIONS PREDICTION*. 2011.

[73] J. C. Wurzenberger, S. Bardubitzki, S. Kutschi, R. Fairbrother, and C. Poetsch, 'Modeling of Catalyzed Particulate Filters - Concept Phase Simulation and Real-Time Plant Modeling on HiL', *SAE International Journal of Engines*, vol. 9, no. 3, pp. 1720–1734, 2016.

[74] H. Lv, J. Li, J. Ling, and M. Wang, 'Research on Diesel Exhaust Aftertreatment System Modelling for Virtual Test Bed', *IOP Conf. Ser.: Earth Environ. Sci.*, vol. 859, no. 1, p. 012082, Sep. 2021, doi: 10.1088/1755-1315/859/1/012082.

[75] K. Parikh, *Three-way catalyst calibration and system modelling for CNG engine exhaust aftertreatment*. 2022. Accessed: Jun. 28, 2023. [Online]. Available: https://urn.kb.se/resolve?urn=urn:nbn:se:kth:diva-314069

[76] G. Brinklow *et al.*, 'Impact of Cylinder Deactivation Strategies on Three-way Catalyst Performance in High Efficiency Low Emissions Engines', *Chemical Engineering Journal Advances*, vol. 14, p. 100481, May 2023, doi: 10.1016/j.ceja.2023.100481.

[77] Chen Danan, Li Jun, Huang Hongyu, Chen Ying, He Zhaohong, and Deng Lisheng, 'Progress in Ammonia Combustion and Reaction Mechanism'.